Supporting Information

Reversible Conversion of Valence-Tautomeric Copper Metal-Organic Frameworks Dependent Single-Crystal-to-Single-Crystal Oxidation/Reduction: Redox-Switchable Catalyst for C–H Bonds Activation Reaction

Chao Huang, Jie Wu*, Chuanjun Song, Ran Ding, Yan Qiao, Hongwei Hou*, Junbiao Chang*, Yaoting Fan

The College of Chemistry and Molecular Engineering, Zhengzhou University, Zhengzhou, Henan, 450052, P. R. China

Contents

1. **General Method.** 1,2,4,5-tetra(2H-tetrazole-5-yl)-benzene (H_4TTB) was synthesized according to a modified procedure from the literature.[1] DIPEA, TEA, and DIEA were distilled from CaH_2, and then dried by 5A molecular sieve. Other reagents and solvents were commercially available and used as received without further purification. ^1H and ^{13}C NMR spectra were obtained with Bruker Avance-400 spectrometers. LC–MS spectra were measured on an Agilent MSD-1100 ESI-MS/MS system. Chemical shifts are reported as δ (ppm) downfield with respect to an internal standard of tetramethylsilane (TMS). FT-IR spectra were recorded on a Bruker-ALPHA spectrophotometer with KBr pellets in 400-4000 cm^{-1} region. Elemental analyses (C, H, and N) were carried out on a FLASH EA 1112 elemental analyzer. X-ray photoelectron spectroscopy (XPS) determination was measured in an ESCALAB 250Xi-type instrument. Inductively coupled plasma atomic emission spectrometry (ICP-AES) analyses were carried out on a Thermo Scientic ICP 6000 spectrometry. Powder X-ray diffraction (PXRD) patterns were recorded using Cu $K\alpha_1$ radiation on a PANalyticalX'Pert PRO diffractometer. Thermal analyses were performed on a Netzsch STA 449C thermal analyzer at a heating rate of 10 °C·min^{-1} in air. A Cary 500 spectrophotometer equipped with a 110 nm diameter integrating sphere was used for collecting diffuse reflectivity spectra of the samples from 200 to 1200 nm. In the measurement process, $BaSO_4$ was selected as a standard with 100 % reflectance. Variable-temperature magnetic susceptibilities were carried out on a SQUID MPMS XL-7 instrument with phase-pure crystalline samples under the applied field of 1 kOe in the temperature region of 2-300 K. Due to its instability in air, the N_2 adsorption and pore size distribution measurements on **1** could not be carried out successfully. The pore size distributions of **2** were collected on a Micromeritics ASAP 2420 Accelerated Surface Area and Porosimetry System under ultrahigh vacuum in a clean system, with a diaphragm and turbo pumping system. Ultrahigh-purity-grade (> 99.999%) N_2 gas was applied in all adsorption measurements. The experimental temperature was maintained by liquid nitrogen (77 K). Prior to measurement, bulk sample of **2** was washed by absolute ethanol (EtOH) three times, dried under vacuum and then transferred into stainless steel column. After 20 min of soaking and venting of supercritical CO_2 (SC-CO_2) by a DB-80 simplex pump, the column pressure regulator was set at 109 bar by soaking SC-CO_2 and the column temperature was raised to 60 °C. SC-CO_2 in the column was gradually vented after 12 h. Although the phase purity of bulk samples of **2** was confirmed using PXRD measurements, removal of the guest solvent molecules to obtain activated materials resulted in the collapse of frameworks, at least in our hands, despite numerous attempts.

2. Synthesis

Synthesis of $\{(H_3O)[Cu_2(CN)(TTB)_{0.5}]\cdot 1.5H_2O\}_n$ (1). A mixture of CuCN (0.018 g, 0.2 mmol), H_4TTB (0.017 g, 0.05 mmol), DMF (2 mL), EtOH (2 mL), $NH_3\cdot H_2O$ (2 mL) and DIPEA (2 mL) was placed in a 25 mL Teflon-lined stainless steel container. The mixture was sealed and heated at 160 °C for three days. After the mixture was cooled to ambient temperature at a rate of 5 °C/h, primrose yellow crystals of **1** were obtained with a yield of 80% (based on Cu). Anal. calcd for $C_6H_7Cu_2N_9O_{2.5}$: C, 19.36 %; H, 1.90 %; N, 33.86 %. Found: C, 19.33 %; H, 1.92 %; N, 33.84 %. IR (KBr, cm^{-1}): 3145 (w), 2774 (vw), 2168 (w), 2104 (vs), 1978 (w), 1647 (s), 1463 (m), 1408 (vs), 1139 (w), 1042 (s), 916 (w), 873 (w), 764 (m) 722 (w).

Synthesis of $\{[Cu^{I}Cu^{II}(TTB)(CN)]\cdot 1.5H_2O\}_n$ (2). Black crystals of compound **2** were obtained by heating primrose yellow crystals of **1** at 100 ºC in atmosphere for 12 h. Anal. calcd for $C_{12}H_8Cu_4N_{18}O_3$: C, 20.40 %; H, 1.14 %; N, 35.69 %. Found: C, 20.37 %; H, 1.16 %; N, 35.67 %. IR (KBr, cm^{-1}): 3621 (vw), 3379 (w), 2168 (w), 2135 (vs), 2044(vw), 1980 (w), 1651(s), 1465 (m), 1419(vs), 1164 (m), 1046 (w), 920 (w), 759 (w), 722 (vw).

Synthesis of $\{(H_3O)[Cu_2(TTB)_{0.5}(CN)]\cdot 2H_2O\}_n$ (1a). Compound **1a** was obtained by immersing **2** in the aqueous solution of ascorboc acid (0.05 mol/L) at room temperature for 12 h. The black crystals of **2** turned to primrose yellow while maintaining their original shapes. Anal. calcd for $C_6H_8Cu_2N_9O_3$: C, 18.90 %; H, 2.11 %; N, 33.06 %. Found: C, 18.93 %; H, 2.07 %; N, 33.09 %. IR (KBr, cm^{-1}): 3145 (w), 2774 (vw), 2168 (w), 2104 (vs), 1978 (w), 1647 (s), 1463 (m), 1408 (vs), 1139 (w), 1042 (s), 916 (w), 873 (w), 764 (m) 722 (w).

Synthesis of $\{(TEAH)[Cu_2(TTB)_{0.5}(CN)]\cdot H_2O\}_n$ (3). Primrose yellow crystals of **3** were obtained under identical condition with that of **1**, expect that TEA was used instead of DIPEA. (85% yield based on Cu). Anal. calcd for $C_{12}H_{19}Cu_2N_{10}O$: C, 32.28 %; H, 4.29 %; N, 31.37 %. Found: C, 32.34 %; H, 4.27 %; N, 31.39 %. IR (KBr, cm^{-1}): 3261 (s), 3046 (w), 2985 (vw), 2110 (vs), 1679 (w), 1464 (m), 1405 (m), 1169 (w), 1041 (m), 910 (m), 834 (w), 791 (vw) 783 (w) 722 (w).

Synthesis of$\{(DIEAH)[Cu_2(CN)(TTB)_{0.5}]\cdot 0.5H_2O\}_n$ (4). Primrose yellow crystals of **4** were obtained under identical conditions with that of **1**, expect that DIEA was used instead of DIPEA. (78% yield based on Cu). Anal. calcd for $C_{12}H_{19}Cu_2N_{10}O$: C, 32.94 %; H, 4.14 %; N, 32.02 %. Found: C, 32.96 %; H, 4.10 %; N, 32.05 %. IR (KBr, cm^{-1}): 3273 (s), 2942 (w), 2867 (vw), 2168 (w), 2110 (s), 1588(vs), 1455 (vs), 1185 (vw), 1084 (vs), 984 (vw), 920 (m), 758 (w), 720 (w).

3. Procedure for the 1-catalyzed direct C–H bonds arylation reaction of heteroarenes. To a solution of DMF (4 mL) charged with heterocycle (1.0 mmol) and aryl halide (2.0 mmol) was added **1** (0.025 mmol), and K_2CO_3 (2.0 mmol). The resulting mixture was stirred at 140 °C and monitored by TLC. After the completion of the reaction (approximately 10 h), the mixture was cooled to room temperature, and diluted with ethyl acetate. The product was then filtered and extracted with brine (3 × 10 mL). The organic phases were combined, dried over anhydrous Na_2SO_4, and concentrated under reduced pressure. The residue was purified by column chromatography on silica gel (*n*-hexanes/ethyl acetate) to give the pure product.

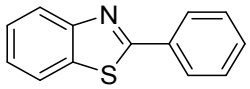

2-Phenylbenzothiazole: Complex **1** (9 mg, 0.025 mmol), benzothiazole (134 mg, 1.0 mmol), iodobenzene (408 mg, 2.0 mmol), K_2CO_3 (276 mg, 2.0 mmol), and DMF (4 mL). After column chromatography (hexanes, then 10% ethyl acetate in hexanes) 190 mg (90%) of a white solid was obtained. This compound had been reported.[2] ^{1}H NMR (400 MHz, $CDCl_3$) δ: 8.04-8.11 (m, 3H), 7.91 (d, *J* = 8.0 Hz, 1H), 7.45-7.51 (m, 4H), 7.37 (t, *J* = 8.0, 1H)

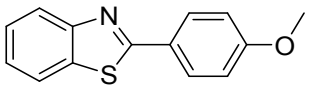

2-(4-methoxyphenyl)benzothiazole: Complex **1** (9 mg, 0.025 mmol), benzothiazole (134 mg, 1.0 mmol), 4-iodoanisole (468 mg, 2.0 mmol), K_2CO_3 (276 mg, 2.0 mmol), and DMF (4 mL). After column chromatography (hexanes, then 10% ethyl acetate in hexanes) 216 mg (91%) of a white solid was obtained. This compound had been reported.[21] H NMR (400 MHz, $CDCl_3$) δ: 7.44 (d, *J* = 8.0 Hz, 1H), 7.14-7.24 (m, 3H), 7.45-7.51 (m, 4H), 6.74-6.86 (m, 4H), 3.79 (s, 3H).

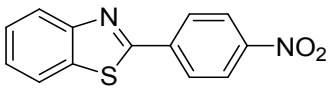

2-(4-Nitro-phenyl)-benzothiazole: Complex **1** (9 mg, 0.025 mmol), benzothiazole (134 mg, 1.0 mmol), 1-iodo-4-nitrobenzene (498 mg, 2 mmol), K_2CO_3 (276 mg, 2.0 mmol), and DMF (4 mL). After column chromatography (hexanes, then 10% ethyl acetate in hexanes) 160 mg (63%) of a yellow solid was obtained. This compound had been reported.[3] ^{1}H NMR (400 MHz, $CDCl_3$) δ: 8.15 (d, *J* = 8.0 Hz, 2H), 8.07 (d, *J* = 8.0 Hz, 2H), 7.97 (d, *J* = 8.0 Hz, 1H), 7.82 (d, *J* = 8.0 Hz, 1H), 7.48 (t, *J* = 8.0 Hz, 1H), 7.39 (t, *J* = 8.0 Hz, 1H).

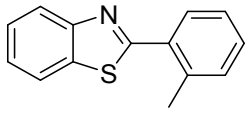

2-o-Tolylbenzothiazole: Complex **1** (9 mg, 0.025 mmol), benzothiazole (134 mg, 1.0 mmol), 2-iodobenzene (436 mg, 2.0 mmol), K_2CO_3 (276 mg, 2.0 mmol), and DMF (4 mL). After column chromatography (hexanes, then 10% ethyl acetate in hexanes) 196 mg (87%) of a light tan solid was obtained. This compound had been reported.[4] ^{1}H NMR (400 MHz, $CDCl_3$) δ: 8.11 (d, *J* = 8 Hz, 1H), 7.94 (d, *J* = 8.0 Hz, 1H), 7.76 (d, *J* = 8.0 Hz, 1H), 7.49-7.56 (m, 1H), 7.30-7.45 (m, 4H), 2.67 (s, 3H).

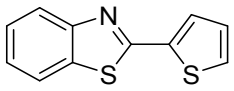

2-(Thiophen-2-yl)benzothiazole: Complex **1** (9 mg, 0.025 mmol), benzothiazole (134 mg, 1.0 mmol), 2-iodothiophene (420 mg, 2.0 mmol), K_2CO_3 (276 mg, 2.0 mmol), and DMF (4 mL). After column chromatography (hexanes, then 10% ethyl acetate in hexanes) 134 mg (62%) of a yellow solid was obtained. This compound had been reported.[5] ^{1}H NMR (400 MHz, $CDCl_3$) δ: 8.01 (d, *J* = 8.0 Hz, 1H), 7.84 (d, *J* = 8.0 Hz, 1H), 7.62-7.66 (m, 1H), 7.43-7.51 (m, 2H), 7.32-7.38 (m, 1H), 7.11-7.14 (m, 1H).

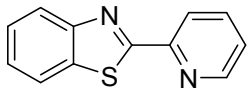

2-(2-Pyridyl)benzothiazole: Complex **1** (9 mg, 0.025 mmol), benzothiazole (134 mg, 1.0 mmol), 2-iodopyridine (410 mg, 2.0 mmol), K_2CO_3 (276 mg, 2.0 mmol), and DMF (4 mL). After column chromatography (hexanes, then 20% ethyl acetate in hexanes) 110 mg (52%) of a white solid was obtained. This compound had been reported.[6] ^{1}H NMR (400 MHz, $CDCl_3$) δ: 8.78 (d, *J* = 8.0 Hz, 1H), 8.32 (d, *J* = 8.0 Hz, 1H), 7.77-7.88 (m, 2H), 7.61-7.66 (m, 1H), 7.33-7.43 (m, 3H).

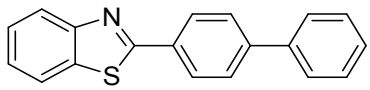

2-(biphenyl-4-yl)benzothiazole: Complex **1** (9 mg, 0.025 mmol), benzothiazole (134 mg, 1.0 mmol), 4-iodobiphenyl (560 mg, 2.0 mmol), K_2CO_3 (276 mg, 2.0 mmol), and DMF (4 mL). After column chromatography (hexanes, then 10% ethyl acetate in hexanes) 146 mg (51%) of a white solid was obtained. This compound had been reported.[3] ^{1}H NMR (400 MHz, $CDCl_3$) δ: 7.46-7.58 (m, 6H), 7.34-7.44 (m, 4H), 7.27-7.31 (m, 1H), 7.07-7.15 (m, 2H).

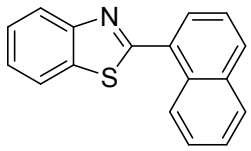

2-(1-Naphthyl)benzothiazole: Complex **1** (9 mg, 0.025 mmol), benzothiazole (134 mg, 1.0 mmol), 2-iodonapthalene (508 mg, 2.0 mmol), K_2CO_3 (276 mg, 2.0 mmol), and DMF (4 mL). After column chromatography (hexanes, then 10% ethyl acetate in hexanes) 122 mg (47%) of a red solid was obtained. This compound had been reported.[7] ^{1}H NMR (400 MHz, $CDCl_3$) δ: 8.92 (d, *J* = 8.0 Hz, 1H), 8.19 (d, *J* = 8.0 Hz, 1H), 7.88-8.01 (m, 4H), 7.51-7.64 (m, 4H), 7.44 (t, *J* = 8.0 Hz, 1H).

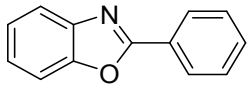

2-Phenylbenzoxazole: Complex **1** (9 mg, 0.025 mmol), benzoxazole (134 mg, 1.0 mmol), iodobenzene (408 mg, 2.0 mmol), K_2CO_3 (276 mg, 2.0 mmol), and DMF (4 mL). After column chromatography (hexanes, then 10% ethyl acetate in hexanes) 178 mg (91%) of a white solid was obtained. This compound had been reported.[8] ^{1}H NMR (400 MHz, $CDCl_3$) δ: 8.05-8.10 (m, 3H), 7.89 (d, *J* = 8.0 Hz, 1H), 7.46-7.50 (m, 4H), 7.37 (t, *J* = 8.0 Hz, 1H)

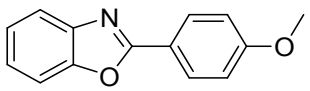

2-(4-methoxyphenyl)benzoxazole: Complex **1** (9 mg, 0.025 mmol), benzoxazole (134 mg, 1.0 mmol), 4-iodoanisole (468 mg, 2.0 mmol), K_2CO_3 (276 mg, 2.0 mmol), and DMF (4 mL). After column chromatography (hexanes, then 10% ethyl acetate in hexanes) 200 mg (89%) of a white solid was obtained. This compound had been reported.[8] ^{1}H NMR (400 MHz, $CDCl_3$) δ: 8.21 (d, *J* = 8.0 Hz, 2H), 7.74 (d, *J* = 8.0 Hz, 1H), 7.55 (d, *J* = 8.0 Hz, 1H), 7.33 (m, 2H), 7.03 (d, *J* = 8.0 Hz, 2H), 3.81 (s, 3H).

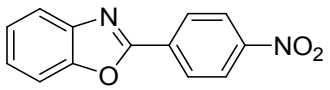

2-(4-Nitro-phenyl)-benzoxazole: Complex **1** (9 mg, 0.025 mmol), benzoxazole (134 mg, 1.0 mmol), 1-iodo-4-nitrobenzene (498 mg, 2.0 mmol), K_2CO_3 (276 mg, 2.0 mmol), and DMF (4 mL). After column chromatography (hexanes, then 10% ethyl acetate in hexanes) 168 mg (70%) of a yellow solid was obtained. This compound had been reported.[9] ^{1}H NMR (400 MHz, $CDCl_3$) δ: 8.29-8.34 (m, 1H), 8.12 (d, *J* = 8.0 Hz, 2H), 7.94 (d, *J* = 8.0 Hz, 1H), 7.85 (d, *J* = 8.0 Hz, 1H), 7.37-7.58 (m, 3H).

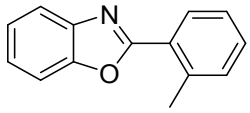

2-o-Tolylbenzoxazole: Complex **1** (9 mg, 0.025 mmol), benzoxazole (134 mg, 1.0 mmol), 2-iodobenzene (436 mg, 2.0 mmol), K_2CO_3 (276 mg, 2.0 mmol), and DMF (4 mL). After column chromatography (hexanes, then 10% ethyl acetate in hexanes) 186 mg (89%) of a light tan solid was obtained. This compound had been reported.[10] ^{1}H NMR (400 MHz, $CDCl_3$) δ: 8.16 (d, J = 8.0 Hz, 1H), 7.77-7.82 (m, 1H), 7.56-7.60 (m, 1H), 7.31-7.43 (m, 5H), 2.88 (s, 3H).

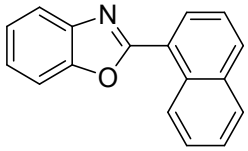

2-(1-Naphthyl)benzoxazole: Complex **1** (9 mg, 0.025 mmol), benzoxazole (134 mg, 1.0 mmol), 2-iodonapthalene (508 mg, 2.0 mmol), K_2CO_3 (276 mg, 2.0 mmol), and DMF (4 mL). After column chromatography (hexanes, then 10% ethyl acetate in hexanes) 110 mg (45%) of a red solid was obtained. This compound had been reported.[11] ^{1}H NMR (400 MHz, $CDCl_3$) δ: 8.42 (d, J = 8.0 Hz, 1H), 8.02 (d, J = 8.0 Hz, 1H), 7.85-7.94 (m, 2H), 7.56-7.75 (m, 5H), 7.34-7.44 (m, 2H).

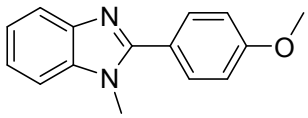

2-(4-Methoxyphenyl)-1-methyl-1*H*-benzo*[d]*imidazole: Complex **1** (9 mg, 0.025 mmol), 1-Methylbenzimidazole (238 mg, 1.0 mmol), 4-iodoanisole (468 mg, 2.0 mmol), K_2CO_3 (276 mg, 2.0 mmol), and DMF (4 mL). After column chromatography (hexanes, then 10% ethyl acetate in hexanes) 138 mg (58%) of a white solid was obtained. This compound had been reported.[12] ^{1}H NMR (400 MHz, $CDCl_3$) δ: 7.76-7.81 (m, 1H), 7.65-7.73 (m, 2H), 7.23-7.38 (m, 3H), 7.00-7.06 (m, 2H), 3.86 (s, 3H), 3.83 (s, 3H).

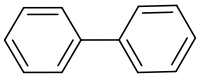

1,1'-biphenyl: Complex **2** (9 mg, 0.025 mmol), benzothiazole (134 mg, 1.0 mmol), iodobenzene (408 mg, 2.0 mmol), K_2CO_3 (276 mg, 2.0 mmol), and DMF (4 mL). After column chromatography (hexanes, then 10% ethyl acetate in hexanes) 109 mg (71%) of a white solid was obtained. This compound had been reported.[13] ^{1}H NMR (400 MHz, $CDCl_3$) δ: 7.46 (d, J = 8.0 Hz, 4H), 7.46 (t, J = 8.0 Hz, 4H), 7.36 (t, J = 8.0 Hz, 2H).

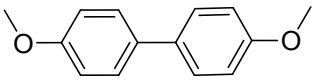

4,4'-dimethoxy-1,1'-biphenyl: Complex **2** (9 mg, 0.025 mmol), benzothiazole (134 mg, 1.0 mmol), 4-

iodoanisole (468 mg, 2.0 mmol), K_2CO_3 (276 mg, 2.0 mmol), and DMF (4 mL). After column chromatography (hexanes, then 10% ethyl acetate in hexanes) 162 mg (76%) of a white solid was obtained. This compound had been reported.[13] ^{1}H NMR (400 MHz, $CDCl_3$) δ: 7.57 (d, J = 8.0 Hz, 4H), 6.93 (d, J = 8.0 Hz, 4H), 3.84 (s, 6H).

4. Crystal Data Collection and Refinement. The data of the **1**, **1a**, and **2-4** were collected on a Rigaku Saturn 724 CCD diffractomer (Mo-*K*α, λ = 0.71073 Å) at temperature of 20 ± 1 °C. Absorption corrections were applied by using numerical program. The data were corrected for Lorentz and polarization effects. The structures were solved by direct methods and refined with a full-matrix least-squares technique based on F^2 with the SHELXL-97 crystallographic software package.[14] The hydrogen atoms were placed at calculated positions and refined as riding atoms with isotropic displacement parameters. There are large solvent accessible void volumes in the crystals of **2** which are occupied by highly disordered free water molecules. No satisfactory disorder model could be achieved, and therefore the SQUEEZE program implemented in PLATON was used to remove these electron densities.[15] The number of solvent molecules were obtained by element analyses and TGA.

Table S1. Crystallographic data and structure refinement details for complexes **1**, **1a**, **2-4**[a,b]

Complex	**1**	**1a**	**2**	**3**	**4**
Formula	$C_6H_7Cu_2N_9O_{2.5}$	$C_6H_8Cu_2N_9O_3$	$C_6H_4Cu_2N_9O_{1.5}$	$C_{12}H_{19}Cu_2N_{10}O$	$C_{12}H_{18}Cu_2N_{10}O_{0.5}$
fw	372.29	382.30	353.26	446.45	437.44
T/K	293(2)	293(2)	293(2)	293(2)	293(2)
λ (Mo K), Å	0.71073	0.71073	0.71073	0.71073	0.71073
Crystal system	monoclinic	monoclinic	monoclinic	monoclinic	monoclinic
Space group	*C2/c*	*C2/c*	*C2/c*	*C2/c*	*Cc*
a (Å)	24.258(5)	24.321(5)	24.338(5)	24.225(5)	24.349(5)
b (Å)	9.4877(19)	9.4098(19)	9.4877(19)	9.6254(19)	9.2334(18)
c (Å)	16.473(3)	16.628(3)	16.502(3)	16.370(3)	16.959(3)
β(°)	118.79(3)	119.24(3)	119.89(3)	118.54(3)	119.41(3)
V (Å^3)	3322.7(12)	3320.7(12)	3303.7(11)	3353.2(12)	3321.5(11)
Z	8	8	8	8	8
$D_{caled.}$(g·cm^{-3})	1.484	1.525	1.420	1.769	1.750
Reflections collected /unique	12534 / 3087	13657 / 3101	3066 / 3066	12471 / 3128	11991 / 4795
abs coeff/mm^{-1}	2.574	2.580	2.581	2.562	2.582
F(000)	1464	1512	1384	1816	1776
θ (°)	1.56-25.50	1.92-25.50	2.35-25.49	1.91-25.50	2.41-25.50
GOF	1.203	1.133	1.162	1.028	1.078
R_1(I>2sigma(I))[a]	0.0539	0.0568	0.0528	0.0543	0.0357
wR_2(I>2sigma(I))[b]	0.1665	0.1751	0.1529	0.1542	0.0879

[a] $R_1 = \sum||F_o|-|F_c||/\sum|F_o|$. [b] $wR_2 = [\sum w(F_o^2 - F_c^2)^2/\sum w(F_o^2)^2]^{1/2}$.

Table S2. Selected Bond Lengths (Å) and Bond Angles (deg) for **1**, **1a**, **2**-**4**

Complex **1**		Complex **2**	
Cu(1)-C(6)	1.930(5)	Cu(1)-C(6)	1.935(3)
Cu(1)-N(2)#1	2.032(4)	Cu(1)-N(2)#1	2.035(2)
Cu(1)-N(7)	2.070(4)	Cu(1)-N(7)#2	2.044(2)
Cu(1)-N(3)#2	2.083(4)	Cu(1)-N(3)	2.076(2)
Cu(2)-N(9)#3	1.902(6)	Cu(2)-N(9)	1.915(3)
Cu(2)-N(5)	2.064(4)	Cu(2)-N(5)	2.066(2)
Cu(2)-N(4)	2.090(4)	Cu(2)-N(4)	2.080(2)
Cu(2)-N(6)#2	2.111(4)	Cu(2)-N(6)#2	2.0990(19)
C(6)-Cu(1)-N(2)#1	115.0(2)	C(6)-Cu(1)-N(2)#1	114.02(11)
C(6)-Cu(1)-N(7)	110.5(2)	C(6)-Cu(1)-N(7)#2	110.69(10)
N(2)#1-Cu(1)-N(7)	112.70(17)	N(2)#1-Cu(1)-N(7)#2	113.35(8)
C(6)-Cu(1)-N(3)#2	114.7(2)	C(6)-Cu(1)-N(3)	115.03(9)
N(2)#1-Cu(1)-N(3)#2	103.94(16)	N(2)#1-Cu(1)-N(3)	104.46(8)
N(7)-Cu(1)-N(3)#2	98.79(16)	N(7)#2-Cu(1)-N(3)	98.19(9)
N(9)#3-Cu(2)-N(5)	129.8(2)	N(9)-Cu(2)-N(5)	130.12(11)
N(9)#3-Cu(2)-N(4)	120.7(2)	N(9)-Cu(2)-N(4)	120.81(10)
N(5)-Cu(2)-N(4)	89.40(16)	N(5)-Cu(2)-N(4)	89.18(8)
N(9)#3-Cu(2)-N(6)#2	114.9(2)	N(9)-Cu(2)-N(6)#2	114.90(9)
N(5)-Cu(2)-N(6)#2	97.23(16)	N(5)-Cu(2)-N(6)#2	97.44(8)
N(4)-Cu(2)-N(6)#2	97.95(16)	N(4)-Cu(2)-N(6)#2	97.20(8)
Complex **1a**			
Cu(1)-C(6)	1.931(4)	Cu(2)-N(9)#3	1.905(5)
Cu(1)-N(3)#1	2.035(4)	Cu(2)-N(8)	2.061(4)
Cu(1)-N(6)#2	2.068(4)	Cu(2)-N(1)	2.087(4)
Cu(1)-N(2)	2.076(4)	Cu(2)-N(7)#2	2.106(4)
C(6)-Cu(1)-N(3)#1	113.43(18)	N(9)#3-Cu(2)-N(8)	130.55(18)

C(6)-Cu(1)-N(6)#2	110.57(19)	N(9)#3-Cu(2)-N(1)	119.55(19)
N(3)#1-Cu(1)-N(6)#2	112.96(16)	N(8)-Cu(2)-N(1)	89.49(15)
C(6)-Cu(1)-N(2)	115.16(18)	N(9)#3-Cu(2)-N(7)#2	115.23(18)
N(3)#1-Cu(1)-N(2)	104.69(14)	N(8)-Cu(2)-N(7)#2	97.03(14)
N(6)#2-Cu(1)-N(2)	99.14(15)	N(1)-Cu(2)-N(7)#2	97.97(15)
Complex **3**			
Cu(1)-N(9)#1	1.913(6)	Cu(2)-C(6)	1.934(4)
Cu(1)-N(8)	2.078(4)	Cu(2)-N(2)#3	2.045(4)
Cu(1)-N(4)	2.094(4)	Cu(2)-N(6)	2.097(4)
Cu(1)-N(7)#2	2.111(4)	Cu(2)-N(3)#2	2.111(4)
N(9)#1-Cu(1)-N(8)	130.55(19)	C(6)-Cu(2)-N(2)#3	117.67(19)
N(9)#1-Cu(1)-N(4)	123.30(19)	C(6)-Cu(2)-N(6)	110.61(19)
N(8)-Cu(1)-N(4)	87.51(16)	N(2)#3-Cu(2)-N(6)	111.20(17)
N(9)#1-Cu(1)-N(7)#2	113.85(18)	C(6)-Cu(2)-N(3)#2	115.72(19)
N(8)-Cu(1)-N(7)#2	96.82(15)	N(2)#3-Cu(2)-N(3)#2	102.14(15)
N(4)-Cu(1)-N(7)#2	97.25(16)	N(6)-Cu(2)-N(3)#2	97.49(16)
Complex **4**			
Cu(1)-N(18)#1	1.953(7)	Cu(3)-N(17)#4	1.919(6)
Cu(1)-N(7)#2	2.073(5)	Cu(3)-N(15)#5	2.030(6)
Cu(1)-N(14)#3	2.089(6)	Cu(3)-N(10)#3	2.033(6)
Cu(1)-N(1)	2.097(5)	Cu(3)-N(6)	2.088(6)
Cu(2)-C(12)	1.889(7)	Cu(4)-C(11)	1.879(7)
Cu(2)-N(3)	2.079(6)	Cu(4)-N(12)#3	2.025(6)
Cu(2)-N(5)	2.088(5)	Cu(4)-N(13)#3	2.058(5)
Cu(2)-N(11)#3	2.096(6)	Cu(4)-N(4)	2.104(6)
N(18)#1-Cu(1)-N(7)#2	112.4(3)	N(17)#4-Cu(3)-N(15)#5	111.4(3)
N(18)#1-Cu(1)-N(14)#3	114.0(3)	N(17)#4-Cu(3)-N(10)#3	113.0(3)
N(7)#2-Cu(1)-N(14)#3	102.8(2)	N(15)#5-Cu(3)-N(10)#3	113.5(2)
N(18)#1-Cu(1)-N(1)	113.3(3)	N(17)#4-Cu(3)-N(6)	114.4(3)

N(7)#2-Cu(1)-N(1)	113.3(2)	N(15)#5-Cu(3)-N(6)	103.7(2)
N(14)#3-Cu(1)-N(1)	99.9(2)	N(10)#3-Cu(3)-N(6)	100.1(2)
C(12)-Cu(2)-N(3)	130.4(3)	C(11)-Cu(4)-N(12)#3	130.2(3)
C(12)-Cu(2)-N(5)	117.5(3)	C(11)-Cu(4)-N(13)#3	117.2(3)
N(3)-Cu(2)-N(5)	89.1(2)	N(12)#3-Cu(4)-N(13)#3	90.7(2)
C(12)-Cu(2)-N(11)#3	117.3(3)	C(11)-Cu(4)-N(4)	115.5(3)
N(3)-Cu(2)-N(11)#3	97.3(2)	N(12)#3-Cu(4)-N(4)	98.1(2)
N(5)-Cu(2)-N(11)#3	98.0(2)	N(13)#3-Cu(4)-N(4)	98.5(2)

Symmetry codes for **1**: #1 = x,-y,z-1/2; #2 = -x,y,-z+1/2; #3 = x,-y+1,z+1/2. Symmetry codes for **2**: #1 = -x+2,-y+2,-z; #2 = -x+2,y,-z+1/2. Symmetry codes for **1a**:#1 = -x+2,-y+2,-z; #2 = -x+2,y,-z+1/2; #3 = -x+2,-y+1,-z. Symmetry codes for **3**: #1 = x,-y+1,z+1/2; #2 = -x,y,-z+1/2; #3 = x,-y,z-1/2. Symmetry codes for **4**: #1 = x,-y+2,z-1/2; #2 = x,-y+1,z-1/2; #3 = x-1/2,-y+3/2,z-1/2; #4 = x,-y+2,z+1/2; #5 = x-1/2,y-1/2,z.

5. Theoretical calculations. The theoretical calculations were performed using the Gaussian 03 suite of program.[16] The unrestricted hybrid density functional UB3LYP method was employed to perform geometrical structure optimization and charge analysis. The mixed basis set including 6-311++G** for Cu and 6-31+G* for C, H, and N was implemented in the calculations.

Table S3. Cartesian coordinates of the optimized structure.

N	22.87997	−0.6011	6.876019
N	21.57196	−0.39088	7.111912
N	21.24459	0.804846	6.674236
N	22.32138	1.405559	6.145343
N	24.31191	3.518079	4.862582
N	25.20075	2.536174	4.594678
N	26.28947	3.073694	4.093136
N	26.14861	4.420486	4.019785
C	23.31352	0.518687	6.284388
C	24.9261	4.656233	4.50191
Cu	19.39116	1.75289	6.801592
N	20.43735	3.359987	3.012311
N	20.60785	3.024787	4.293526
N	19.51683	2.458535	4.765351
N	18.5821	2.405558	3.813244
C	19.18308	2.964408	2.753665
C	18.79469	3.355268	7.743512
Cu	21.1891	7.735456	7.634396
N	20.14337	6.128319	11.42404
N	19.9727	6.463514	10.14284
N	21.06363	7.02983	9.670886
N	21.99848	7.082852	10.62288
N	22.01886	5.152164	6.092378
C	21.39763	6.523982	11.68254
C	21.78565	6.132985	6.69275
Cu	18.24363	6.168595	8.955227
N	17.7001	10.08886	7.559249
N	19.00812	9.878816	7.323361
N	19.3358	8.68337	7.76158
N	18.25918	8.082693	8.290897
N	16.26868	5.970178	9.573823
N	15.37975	6.952013	9.841681
N	14.29128	6.414477	10.34378
N	14.43243	5.067745	10.41757
C	17.26683	8.969255	8.151452
C	15.65482	4.832048	9.935138
Cu	22.337	3.31965	5.481003

N	18.56153	4.336016	8.344026
N	18.20934	0.177641	7.425155
N	17.68347	-0.73692	6.624692
N	16.97746	-1.60032	7.369949
N	17.87009	-0.04719	8.704391
C	17.11713	-1.14655	8.628598
H	16.66517	-1.61839	9.492692
H	18.70287	3.091117	1.791723
H	24.47223	5.631768	4.603644
H	24.3159	0.710099	5.929092
H	16.26452	8.777794	8.506912
H	16.10885	3.856565	9.833611
N	22.37146	9.310578	7.011458
C	23.46575	10.63381	5.808829
H	23.91931	11.10488	4.945154
N	22.71317	9.534224	5.732657
N	22.89556	10.22607	7.812027
N	23.60285	11.08886	7.0673
H	21.87796	6.397305	12.64443

Table S4. Comparison of selected bond lengths (Å) of optimized by DFT calculations with experimental X-ray Diffraction Data. The calculated bond lengths for **2** are in good agreement with the experimental X-ray crystal structure, indicating that our calculated results are reasonable.

Bond	X-ray structure(Å)	Optimized structure(Å)
N9—C6	1.128	1.173
Cu1—C6	1.935	1.952
Cu1—N2	2.035	2.066
Cu1—N3	2.076	2.159
Cu2—N4	2.080	2.118
Cu2—N5	2.066	2.079
Cu2—N6	2.099	2.026
Cu1—N7	2.044	2.086

6. Additional structure figures and characterizations of Cu-complexes

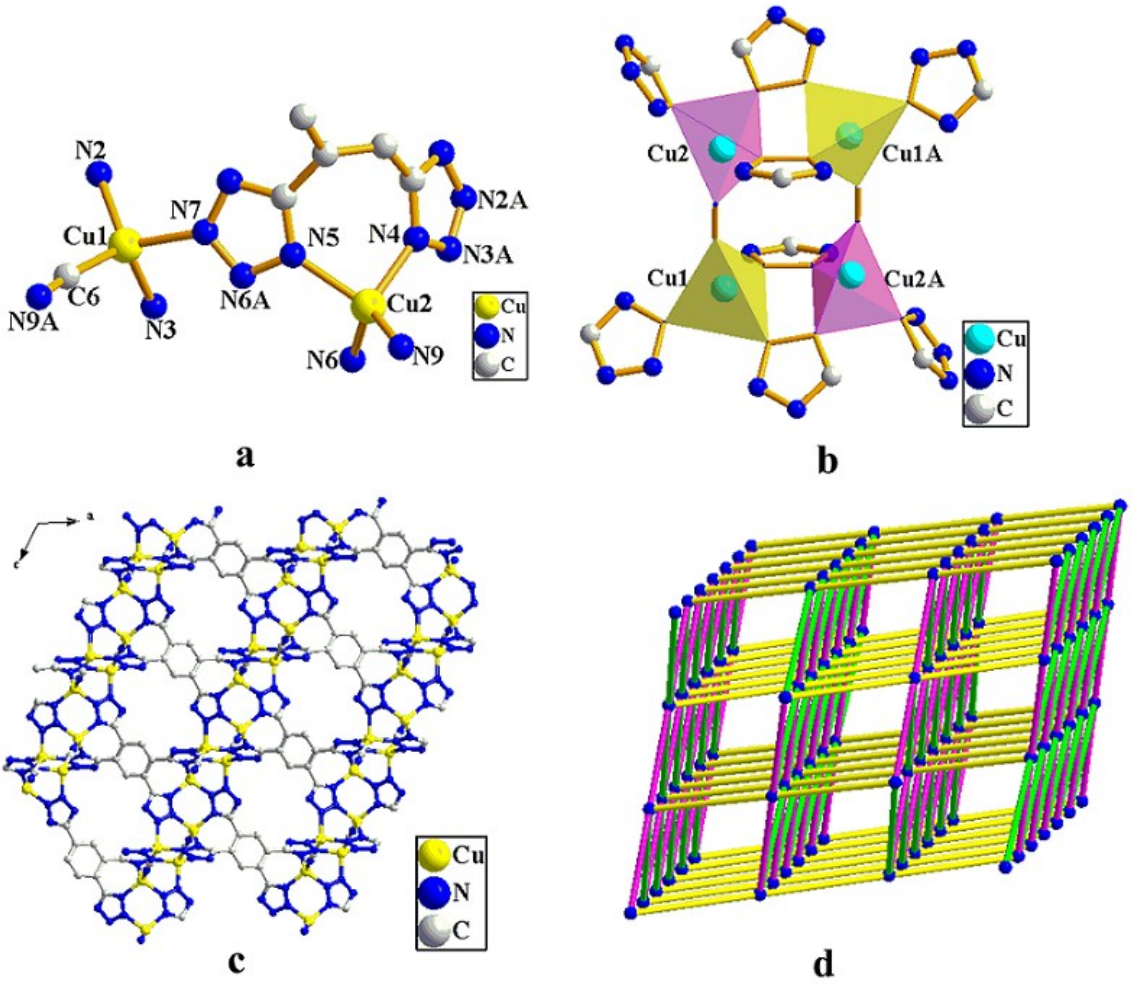

Figure S1. Crystal structure of **1**: (a) coordination environments of the Cu(I) ions. Hydrogen atoms and water molecule are omitted for clarity. (b) The tetranuclear Cu(I) cluster. (c) View of the 3D network of **1** down *b* axis. (d) Schematic view of the $\{4^{10}.6^5\}_2$ topology (the tetranucler Cu(I) cluster respresented as blue ball mode).

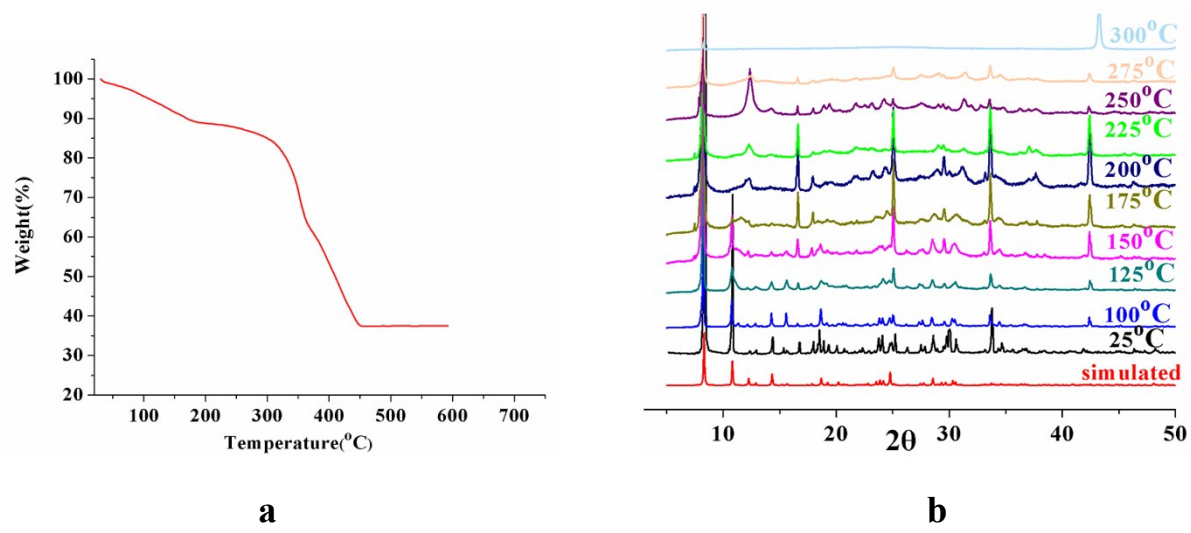

Figure S2. (a) The TG curve of **1**. (b) Variable-temperature PXRD patterns of **1**.

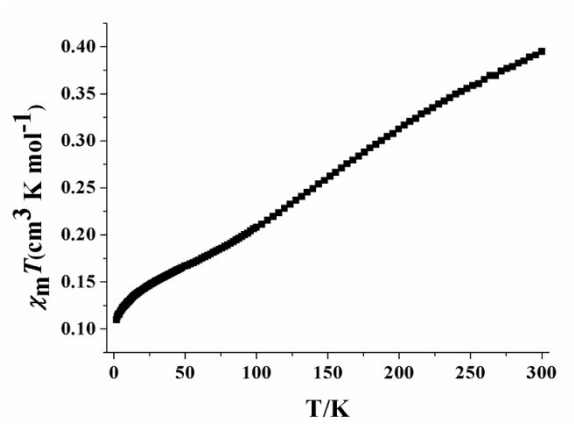

a **b**

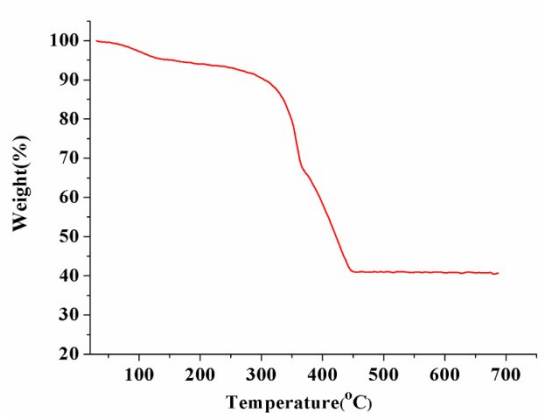

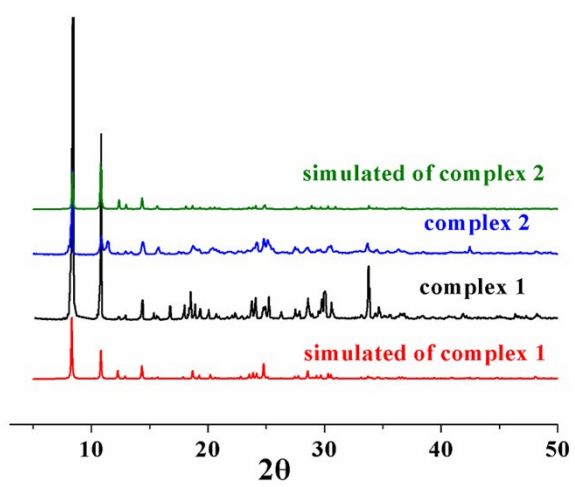

c **d**

Figure S3. (a) Optical microscopic photograph showing the crystals of **2**. (b) $\chi_M T$ vs T plot for **2**. (c) The TG curve of **2**. (d) PXRD patterns of **2** and **1**.

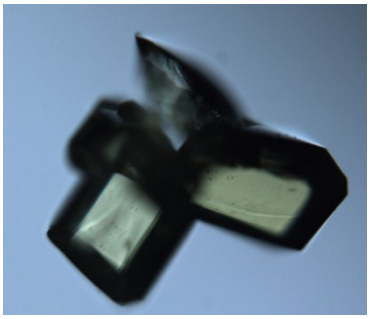

a

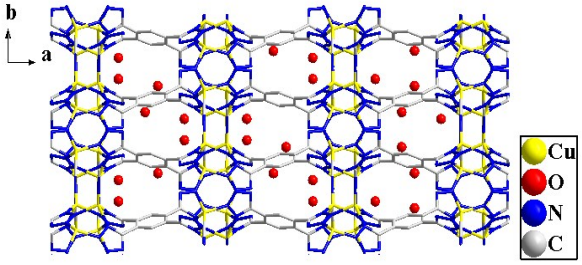

b

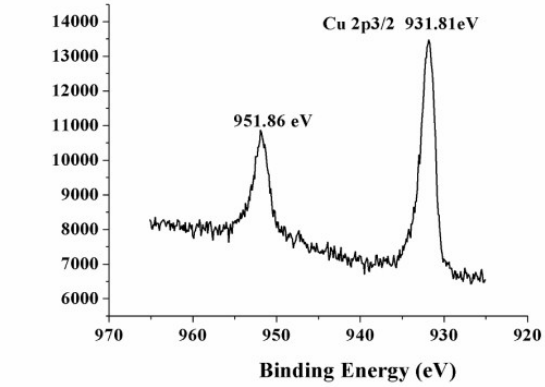

c

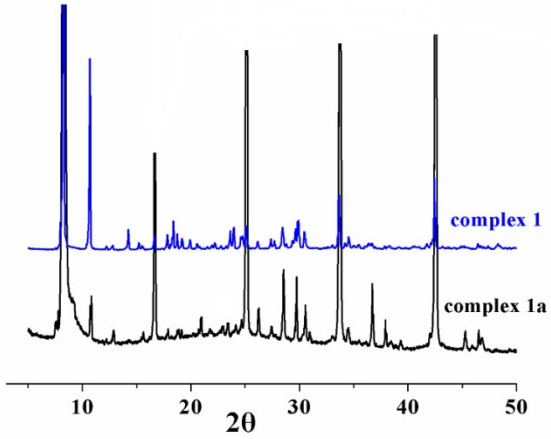

d

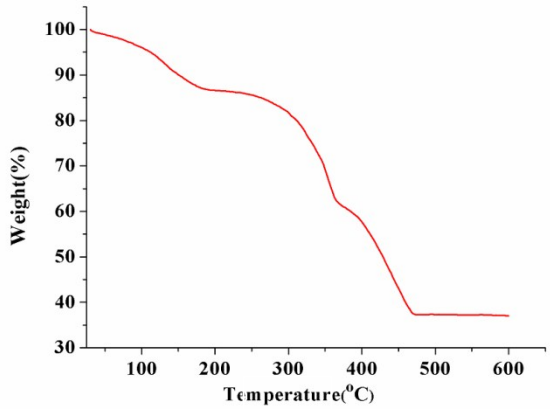

e

Figure S4. (a) Optical microscopic photograph of **1a**. (b) View of the 3D network of compound **1a** down *c* axis. Hydrogen atoms and water molecule are omitted for clarity. (c) XPS spectrum of **1a**. (d) Comparison of PXRD patterns of **1a** and **1**. (e) The TG curve of **1a**.

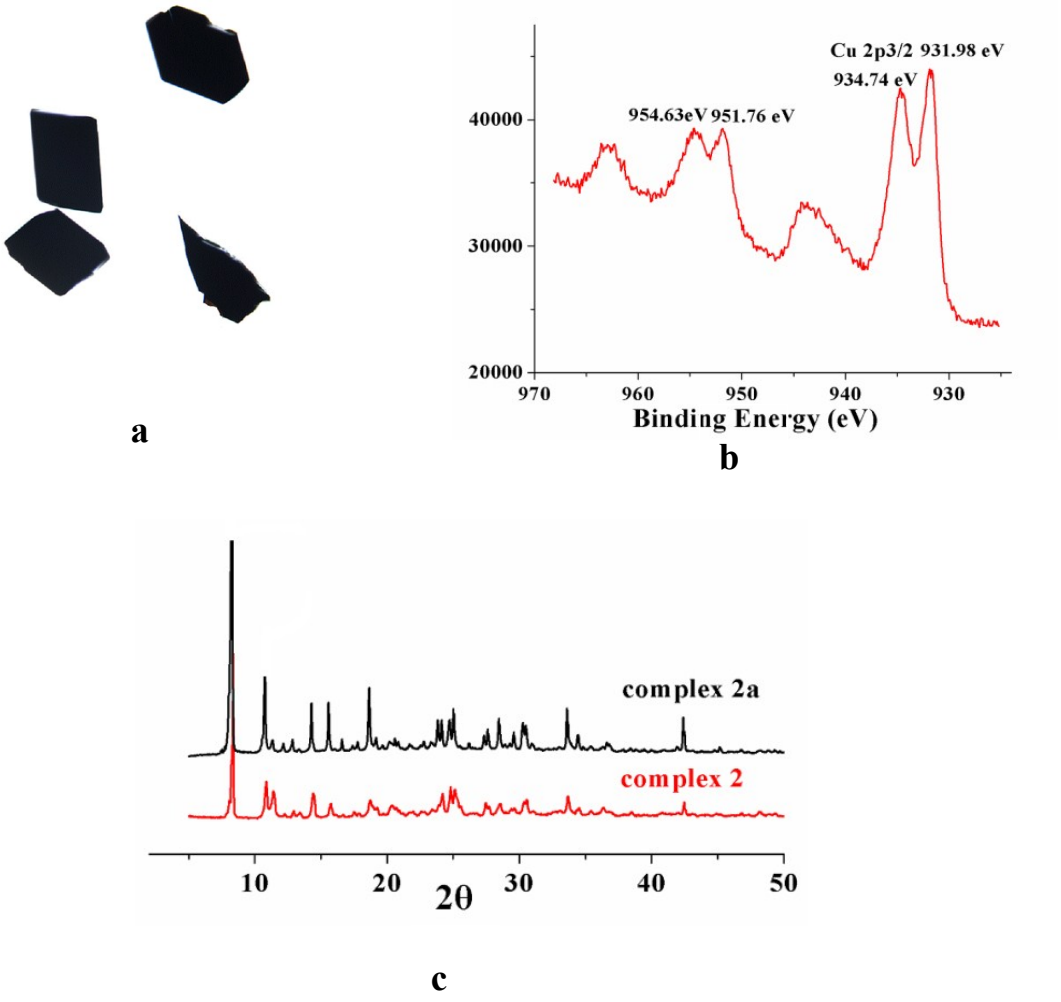

Figure S5. (a) Optical microscopic photograph of **2a**. (b) XPS spectrum of **2a**. (c) Comparison of PXRD patterns of **2a** and **2**.

7. Mechanistic Investigations of Oxidation/Reduction Behavior

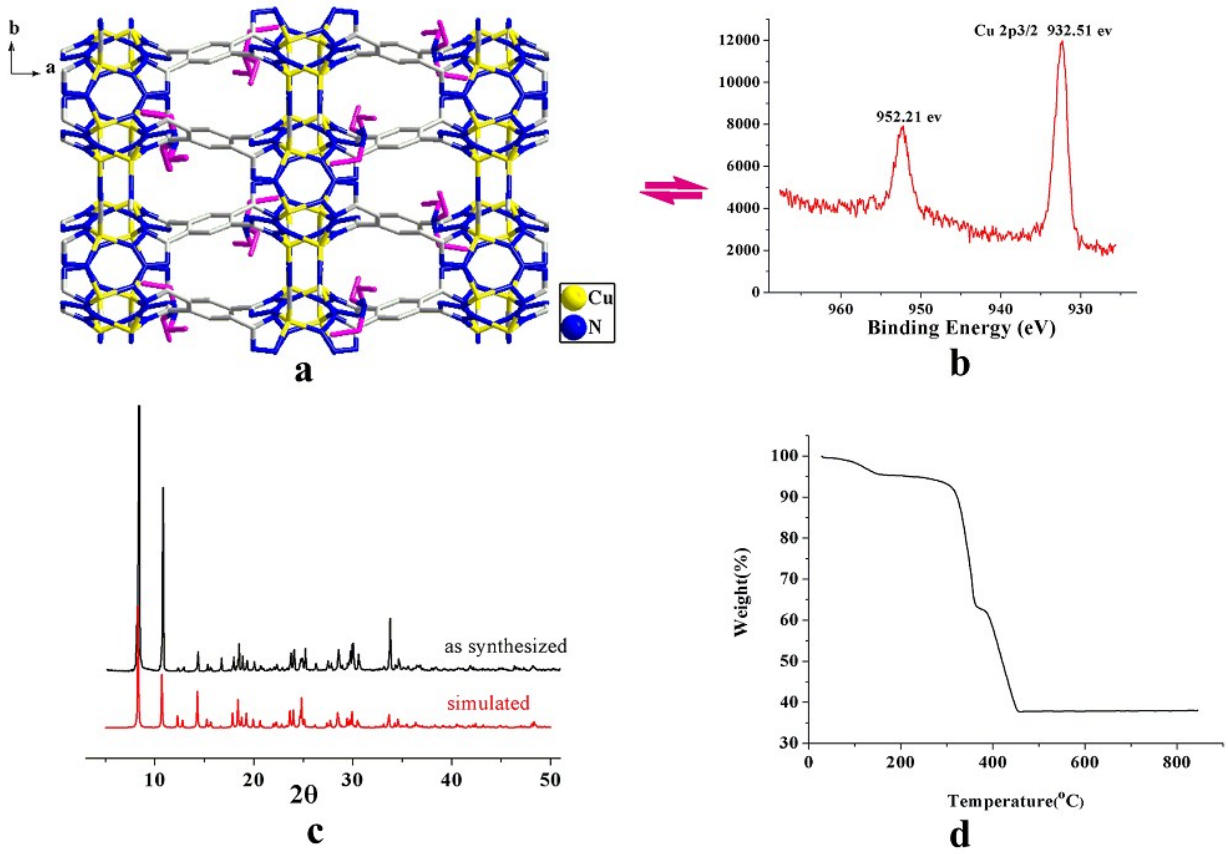

Figure S6. (a) View of the 3D network of compound **3** down *c* axis. Hydrogen atoms and water molecule are omitted for clarity. (b) XPS spectrum of **3**. (c) Simulated and experimental PXRD patterns of **3**. (d) The TG curve of **3**.

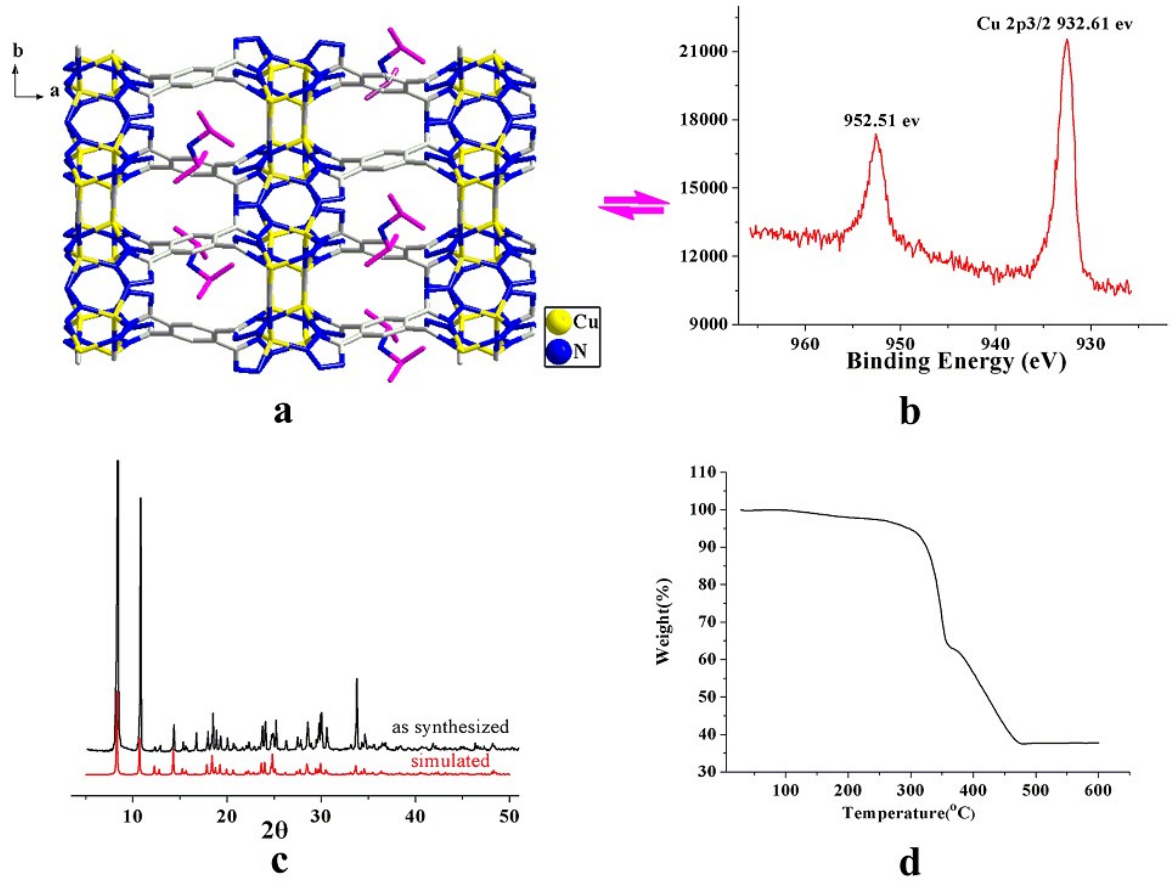

Figure S7. (a) View of the 3D network of compound **4** down *c* axis. Hydrogen atoms and water molecule are omitted for clarity. (b) XPS spectrum of **4**. (c) Simulated and experimental PXRD patterns of **4**. (d) The TG curve of **4**.

In order to understand the influence of guests on the redox behavior of the anionic framework, with triethylamine (TEA) and diisopropylamine (DIPA) as OSDAs, Cu^{I} complexes $\{(TEAH)[Cu^{I}_2(CN)(TTB)_{0.5}]\cdot H_2O\}_n$ (**3**) and $\{(DIPAH)[Cu^{I}_2(CN)(TTB)_{0.5}]\cdot 0.5H_2O\}_n$ (**4**) were obtained, respectively (Figures S6 and S7). Single-crystal X-ray diffraction analysis revealed that **3** and **4** exhibit the identical anionic, porous zeolite-like 3D framework to that of **1** except with $TEAH^+$ or $DIPAH^+$ as guest cations. It is worth noting that without DIPEA, TEA, and DIPA as OSDAs for the synthesis of **1**, **3** and **4**, respectively, none of them could be obtained successfully. The DIPEA cations are too bulky to be accommodated in the framework and hydrated proton guests lie inside the cavity of **1**.

The Cu^{I} complex **1** with hydrated protons as guests can be oxidized to $Cu^{I}Cu^{II}$ mixed-valent complex **2**. In contrast, Cu^{I} complexes **3** and **4** with $TEAH^+$ and $DIPAH^+$ cations as guests, respectively, are relatively stable, remaining unchanged after kept in the air for several months. Therefore, the anionic framework displays

distinct redox behavior depending on the nature of the guests. We assumed that the $[H_3O]^+$ ions encapsulated in the anion-charged Cu^I framework of **1** can be directly involved in the oxidation processes and show higher reactivity than $TEAH^+$ and $DIPAH^+$ cations, thus facilitating to alter the framework charge. On the basis of the above discussions, guest dependent redox activity for the anionic framework may be speculated. Firstly, it is well known that multinuclear Cu^I precursors have been proven to be able to capture O_2 molecules and the predominant roles of most Cu enzymes are O_2 activation.[17] The bulky ammonium cations in **3** and **4** display good adaptability to the cavity of the anionic framework, thereby stabilizing the framework and protecting the Cu^I ions against O_2 attack. In contrast, hydrated proton guests lie inside the cavity of **1**, leaving a partial cavity and Cu^I ions free to capture O_2 molecules. Secondly, the reactions of Cu^I complexes with O_2 take place. According to a generally accepted pathway for the reaction of Cu^I complex with O_2,[17] the $Cu1^I$ ion in **1**, which was more likely to be oxidized than $Cu2^I$ ion, was oxidized to $Cu1^{II}$ ion by O_2 giving rise to a $Cu1^{II}$-($O_2^{-\bullet}$) superoxo species that further linked with the neighboring $Cu1^I$ ions (Cu1···Cu1 3.82 Å) to produce a Cu_2O_2 peroxo species. The peroxo species react with hydrated protons to generate **2** and release H_2O_2. Therefore the oxidation transformation reaction could be described as [Eq. (1)].

$$2\{(H_3O)[Cu^I_2(CN)(TTB)_{0.5}]\cdot 1.5H_2O\}_n\ (\mathbf{1}) + n\ O_2 \longrightarrow 2\{[Cu^ICu^{II}(CN)(TTB)_{0.5}]\cdot 1.5H_2O\}_n\ (\mathbf{2}) + n\ H_2O_2 + 2n\ H_2O \qquad (1)$$

We reasoned that the host-guest dependent oxidation process of **1** could favour the transformation into **2** without reassembly of metal coordination sphere, metal-ligand connectivity and network topology. As a result, the crystallinity of **2** was retained. The subtle variances between **1** and **2** (*e.g.*, bond lengths and angles differences) could also make it practicable of reducing **2** through a SCSC process and subsequently implement the reversible SCSC redox structural transformations.

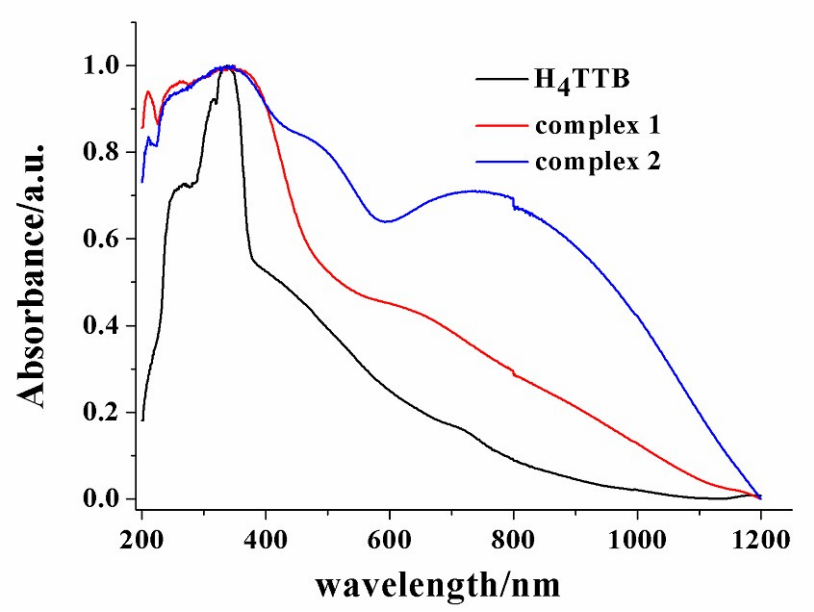

Figure S8. UV-vis absorption spectra at room temperature for the free organic ligand, complexes **1** and **2**.

8. **1**-Catalyzed C–H Arylation.

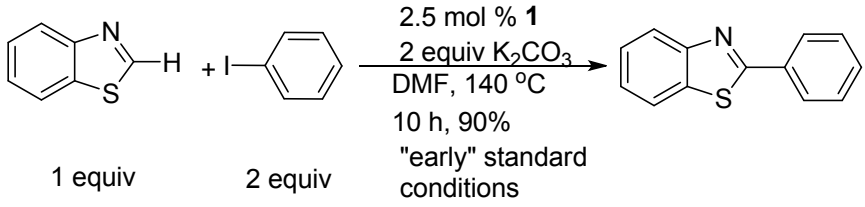

Variation from the "best" standard conditions (isolated yield)

Cu Source	Base	Solvent
without Cu (0)	KO^{t}Bu (< 5%)	acetonitrile (reflux) (< 5%)
CuI (28%)	NaO^{t}Bu (< 5%)	dioxane (reflux) (< 5%)
CuI (90%)[a]	MeONa (< 5%)	toluene (reflux) (< 5%)
CuI/Phen (40%)[b]	$CsCO_3$ (32 %)	NMP (< 5%)
	K_3PO_4 (46%)	diglyme (< 5%)
	Na_2CO_3 (63%)	DMA (58%)
	LiO^{t}Bu (87%)	

Scheme S1. Discovery of **1** Catalysis and Influence of Parameters. [a]Reactions were carried out using CuI (10 mol%), LiO^{t}Bu (2 equiv), benzothiazole (1 equiv) and iodobenzene (3 equiv) in DMF at 140 °C for 10 min. [b]Reactions were carried out using CuI (20 mol%), 1,10-phenanthroline (20 mol%), K_2CO_3 (2 equiv), benzothiazole (1 equiv) and iodobenzene (2 equiv) in DMF at 140 °C for 10 h.

The solvent resistance property and redox stability of **1** in DMF was examined by suspending the single crystal samples in boiling DMF for 48 h because DMF would be chosen as reaction solvent in the catalytic reaction. It was found that the single crystal samples of **1** could remain stable and keep original shapes in boiling DMF for more than 48 h. Single crystal X-ray diffraction showed the unit cell parameters of **1** after treatment basically did not change. Then, the optimization of the reaction conditions for **1**-catalyzed C–H arylation reaction was performed using benzothiazole and iodobenzene as coupling partners (Scheme 1). After extensive screening of solvents, temperature and bases, the standard conditions were obtained using two equivalent of K_2CO_3 as the base in the presence of 2.5 mol % of crystal samples of **1** in DMF at 140 °C for 10 h, giving the desired arylation product in 90% yield. Attempts to replace K_2CO_3 with Na_2CO_3, Cs_2CO_3 or K_3PO_4 resulted in incomplete consumption of substrates and the product was obtained in poor to moderate yield (32-63%). With stronger base such as KO^{t}Bu, NaO^{t}Bu and MeONa, only a trace amount of the desired compound was produced. LiO^{t}Bu, which was the optimal base for *C*-arylation of heterocycles with aryl iodides in the Daugulis system,[18] could also generate the desired product in excellent yield (87%). The coupling proceeded moderately effective in DMA (58%), but diglyme, NMP, acetonitrile, dioxane and toluene were unsuitable solvents. In view of efficiency, cost, simplicity and stability, we identified **1**/K_2CO_3/DMF/140°C as our standard conditions for the cross-coupling reactions.

Table S5. Scope of 1-Catalyzed C–H Arylation.[a]

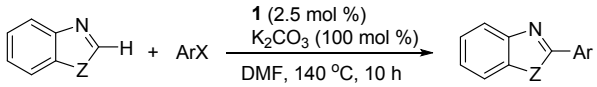

Entry	ArX	Product	Yield (%)[c]
1		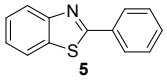 **5**	90
2	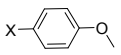	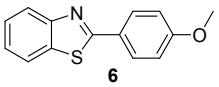 **6**	X = I 91 X = Br 71[b]
3	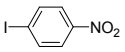	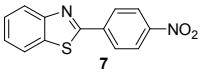 **7**	63
4		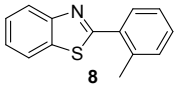 **8**	87
5		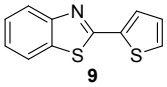 **9**	X = I 62 X = Br 44
6		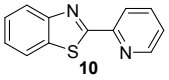 **10**	X = I 52 X = Br 39
7	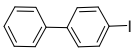	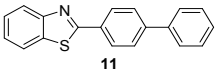 **11**	51[b]
8		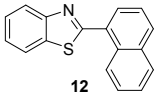 **12**	47[b]
9		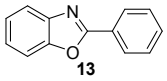 **13**	91
10	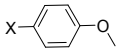	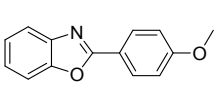 **14**	X = I 89 X = Br 69[b]
11	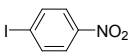	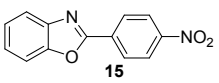 **15**	70

12		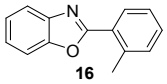 **16**	89
13	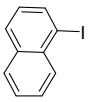	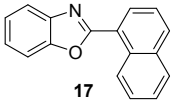 **17**	45[b]
14	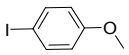	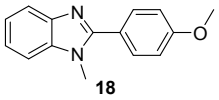 **18**	58

[a]Reaction conditions: heterocycle (1 mmol), aryl halide (2 mmol), complex **1** (2.5 mol %), K_2CO_3 (2 mmol), DMF (4 mL), 140 °C, 10 h. [b]Isolated yield of the product after 24 h. [c]Isolated yield.

Complex **1** catalytic system was found to be general for the coupling of heteroarenes with a variety of substituted aryl or heteroaryl halides, and the results were summarized in Table S4. Electron-rich benzothiazole and benzoxazole were excellent coupling partners, while 1-methylbenzimidazole was much less reactive (compare entries 2, 10, and 14), which may arise from the different acidities of hydrogen at *C*-2 of the heterocycles.[19] In general, the introduction of an electron-donating group on the phenyl ring of iodobenzene led to higher arylation yields than that with an electron-withdrawing group (entries 2 vs. 3, 10 vs. 11). Not surprisingly, aryl bromide was less reactive than the aryl iodide (entries 2 and 10). As an example, the sterically hindered *o*-tolyl iodide also participated in coupling processes with the 2-positions of benzothiazole and benzoxazole to give the respective products **8** and **16** in high efficiency (entries 4 and 12). Reaction of 4-iodobiphenyl with benzothiazole under the conditions of direct C–H bond arylation only resulted in the formation of **11** in 51% isolated yield after 20 h (entry 7), which may due to the fact that the substrate is bulky and it's structure is not in accordance with the geometry of the active center. To further investigate the effect of the substrate size in this reaction, 1-iodonaphthalene was reacted with benzothiazole and benzoxazole, respectively, which gave **12** and **17** in poor isolated yield even after prolonged reaction time (entries 8 and 13). By contrast, reaction of 1-iodonaphthalene with benzothiazole using homogeneous Daugulis system resulted in the formation of **12** in 90% isolated yield.[18] The results clearly indicated that in the heterogeneous catalyst **1** system, the bulky substrate could not easily access the catalytic sites in the framework due to its large diameter, leading to a decline of reaction rate. Heteroaryl halides also underwent reactions with benzothiazole to generate the desired coupling products **9** and **10** in moderate yields (entries 5 and 6).

9. Recycling test for directing heterocycle C-H arylation reaction with 1 and 2.

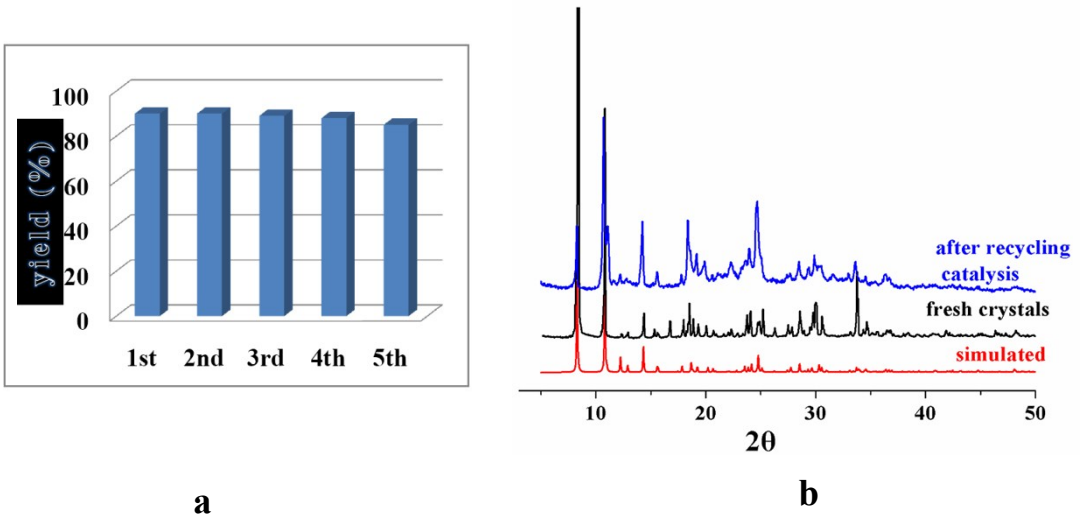

Figure S9. (a) Recycling test for directing heterocycle C-H arylation reaction with **1**. (b) Comparison of the PXRD patterns of **1** before and after catalysis.

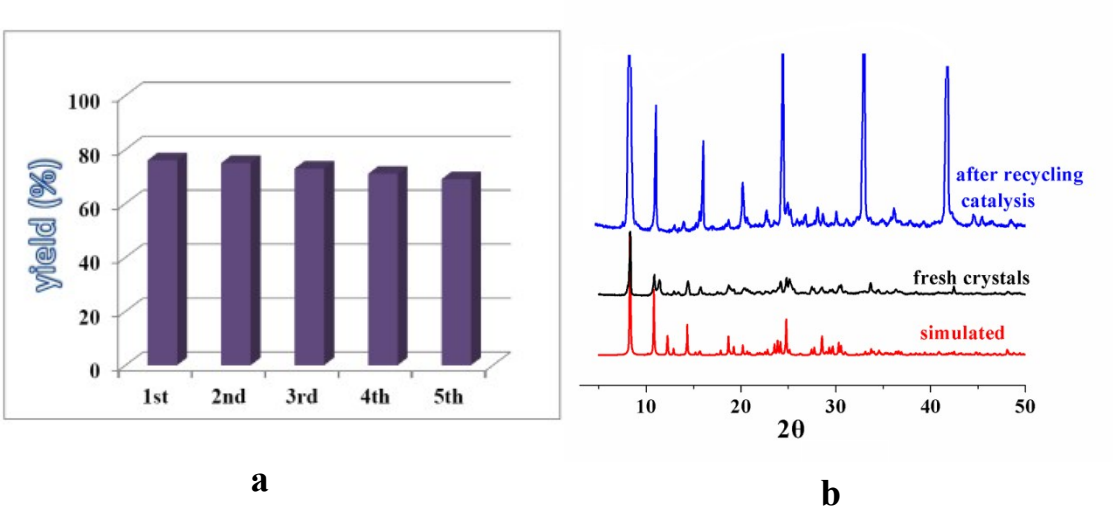

Figure S10. (a) Recycling test for Ullmann coupling reaction with **2**. (b) Comparison of the PXRD patterns of **2** before and after catalysis.

10. Spectral copies of ^{1}H NMR of compounds obtained in this study.

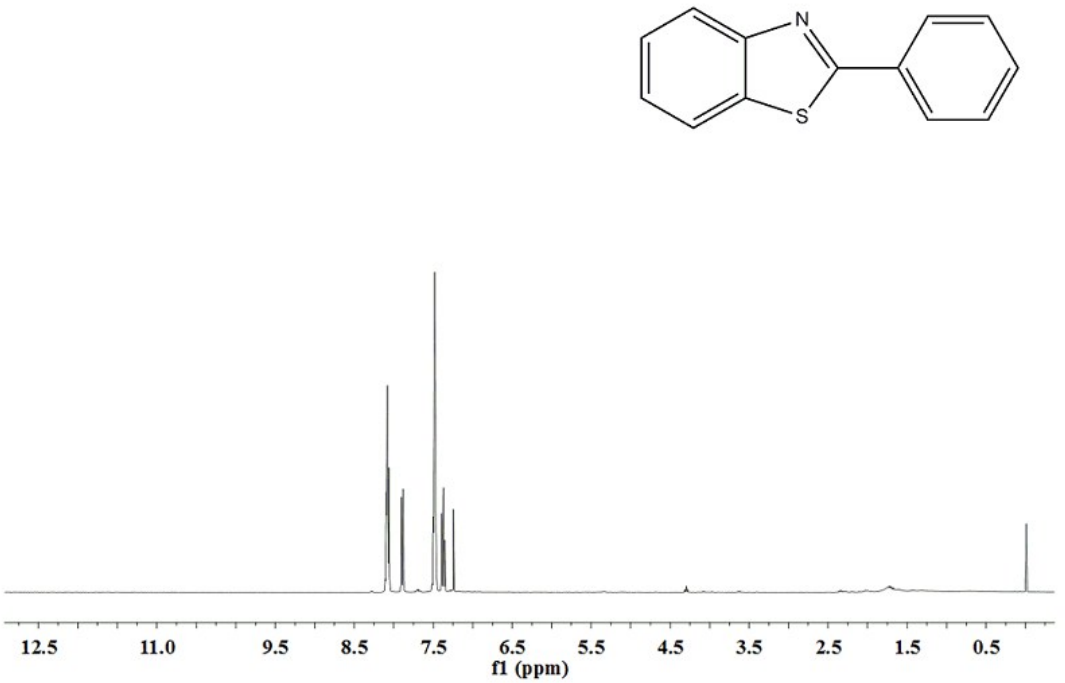

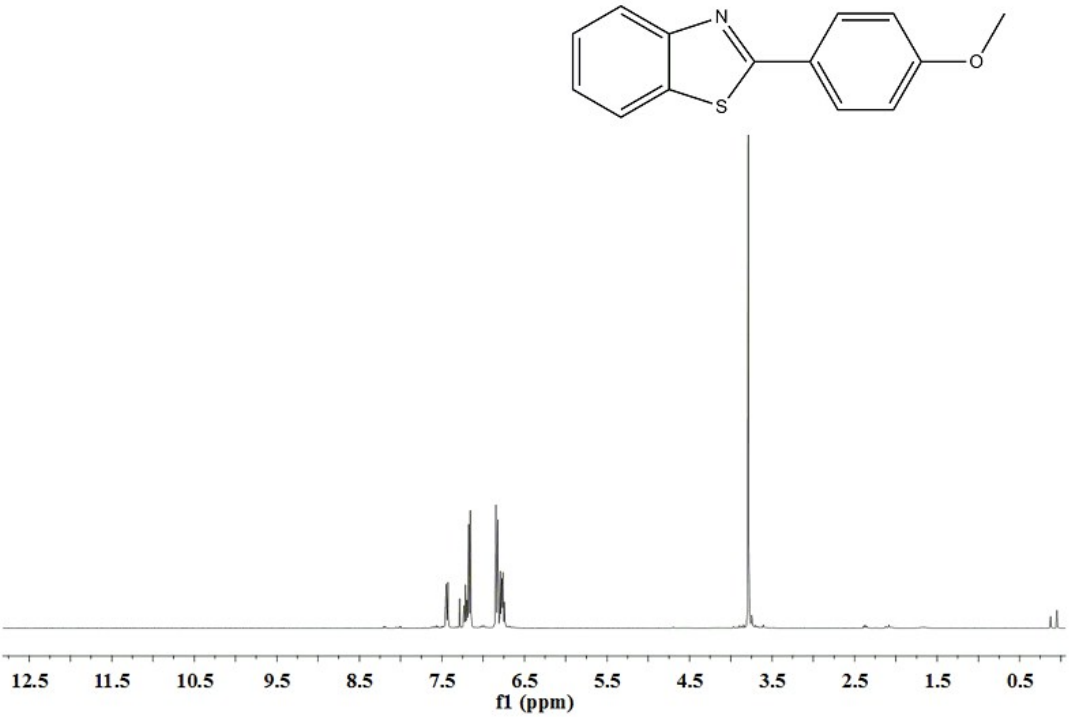

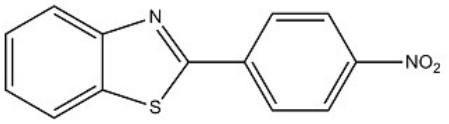
N
S
NO2

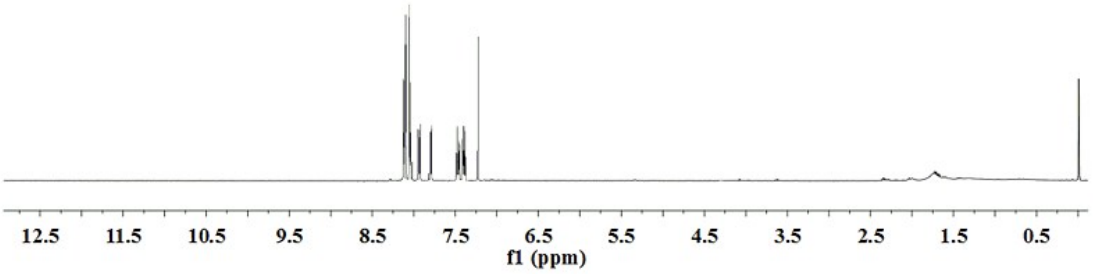
12.5
11.5
10.5
9.5
8.5
7.5
6.5
5.5
4.5
3.5
2.5
1.5
0.5
f1 (ppm)

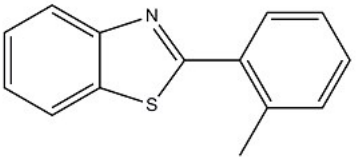
N
S

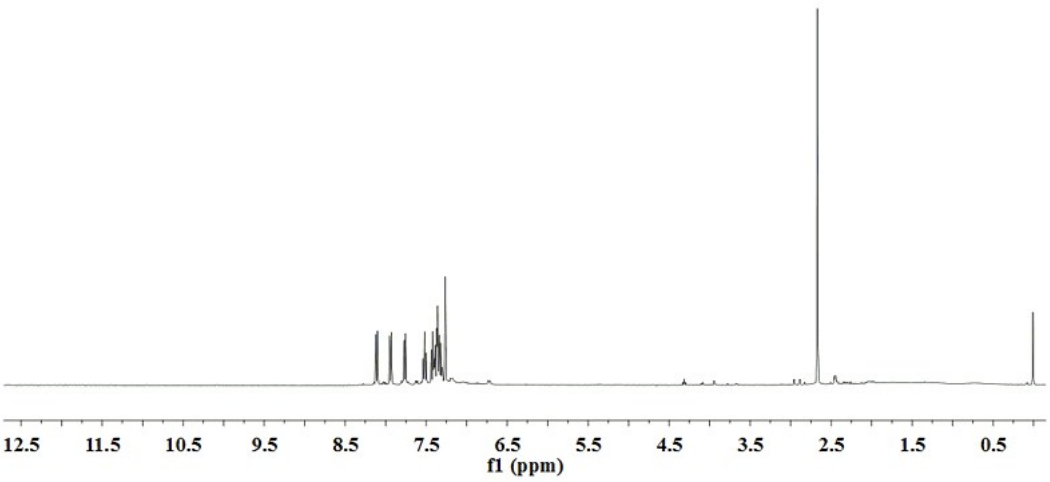
12.5
11.5
10.5
9.5
8.5
7.5
6.5
5.5
4.5
3.5
2.5
1.5
0.5
f1 (ppm)

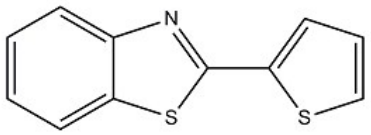
N
S
S

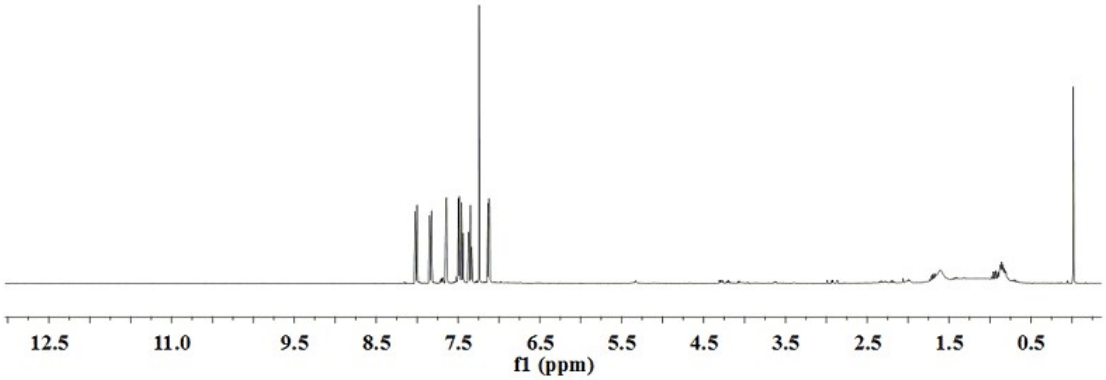
12.5
11.0
9.5
8.5
7.5
6.5
5.5
4.5
3.5
2.5
1.5
0.5
f1 (ppm)

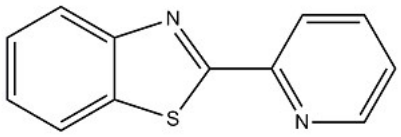
N
S
N

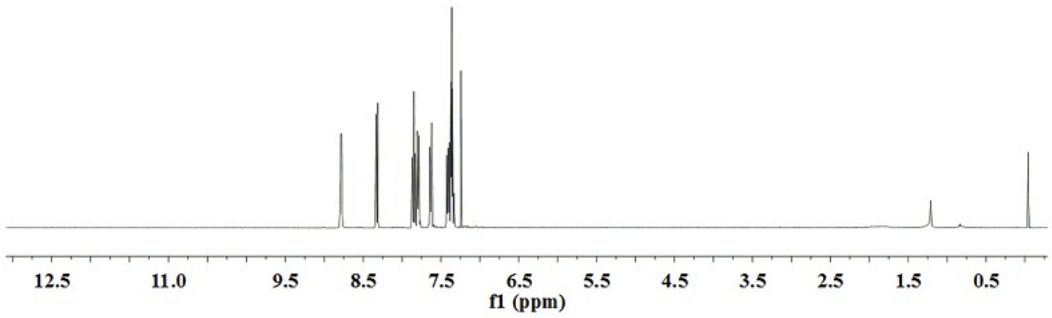
12.5
11.0
9.5
8.5
7.5
6.5
5.5
4.5
3.5
2.5
1.5
0.5
f1 (ppm)

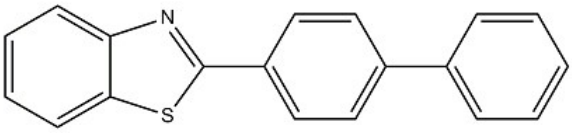
N
S

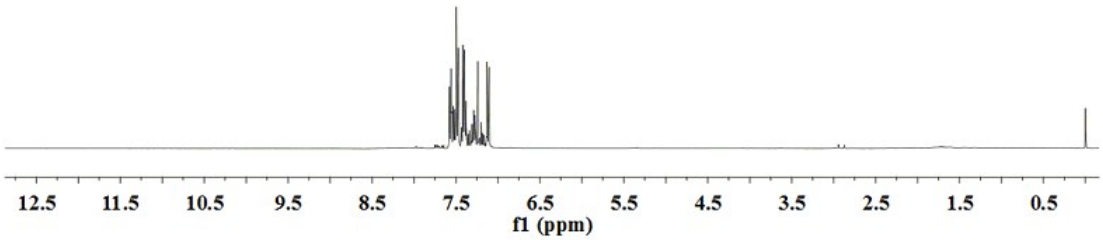
12.5
11.5
10.5
9.5
8.5
7.5
6.5
5.5
4.5
3.5
2.5
1.5
0.5
f1 (ppm)

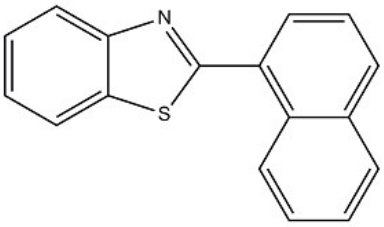
N
S

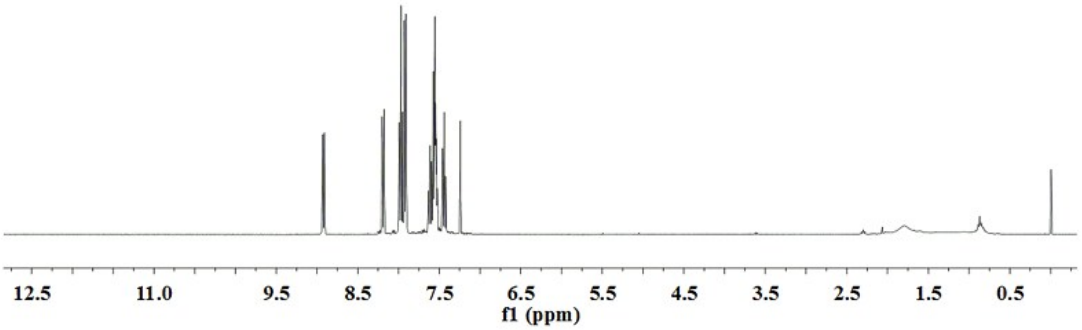
12.5
11.0
9.5
8.5
7.5
6.5
5.5
4.5
3.5
2.5
1.5
0.5
f1 (ppm)

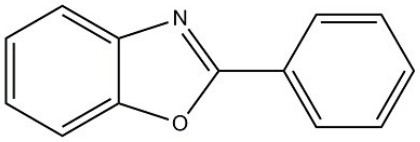
N
O

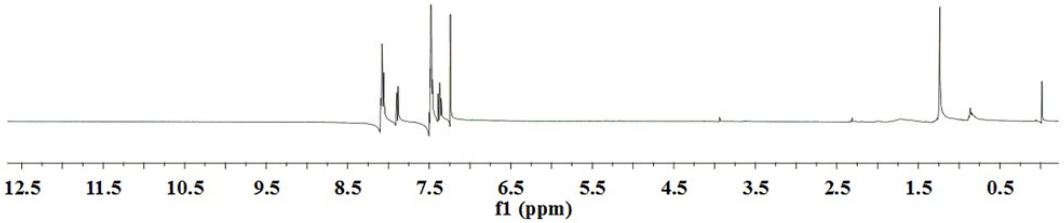
12.5
11.5
10.5
9.5
8.5
7.5
6.5
5.5
4.5
3.5
2.5
1.5
0.5
f1 (ppm)

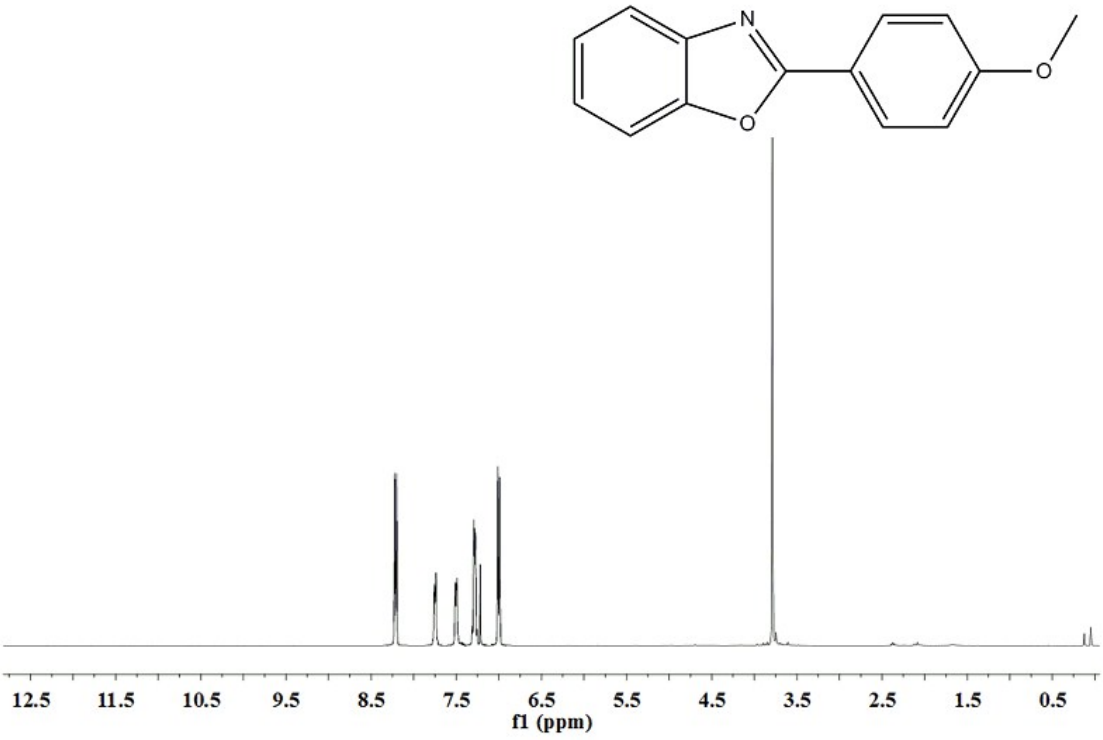
N
O
O
12.5
11.5
10.5
9.5
8.5
7.5
6.5
5.5
4.5
3.5
2.5
1.5
0.5
f1 (ppm)

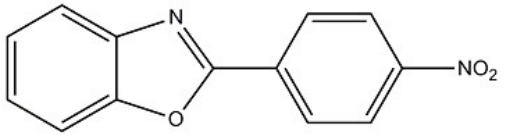
N
O
NO2

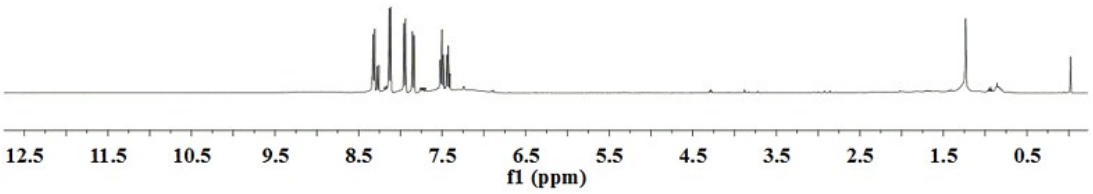
12.5
11.5
10.5
9.5
8.5
7.5
6.5
5.5
4.5
3.5
2.5
1.5
0.5
f1 (ppm)

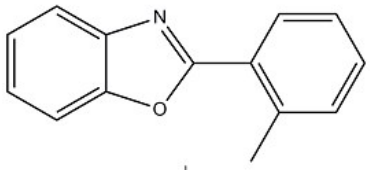
N
O

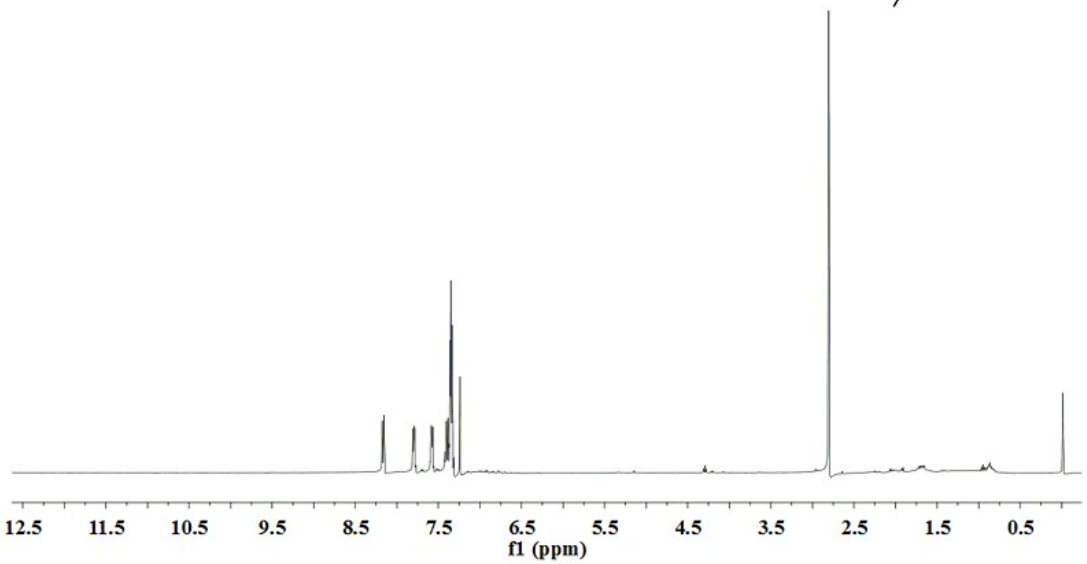
12.5
11.5
10.5
9.5
8.5
7.5
6.5
5.5
4.5
3.5
2.5
1.5
0.5
f1 (ppm)

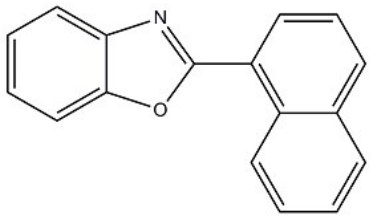
N
O

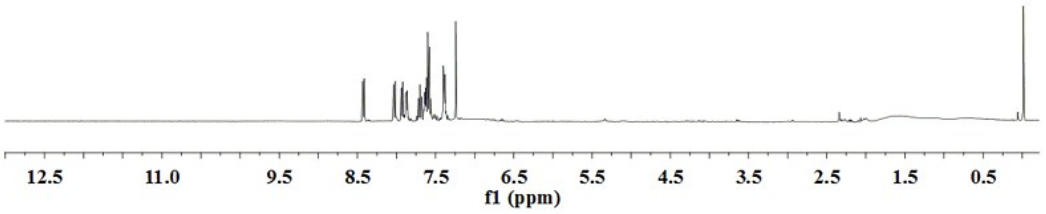
12.5
11.0
9.5
8.5
7.5
6.5
5.5
4.5
3.5
2.5
1.5
0.5
f1 (ppm)

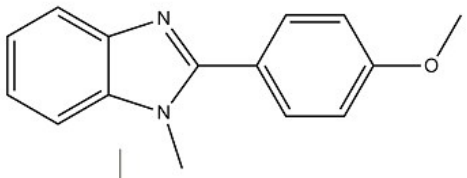
N
N
O

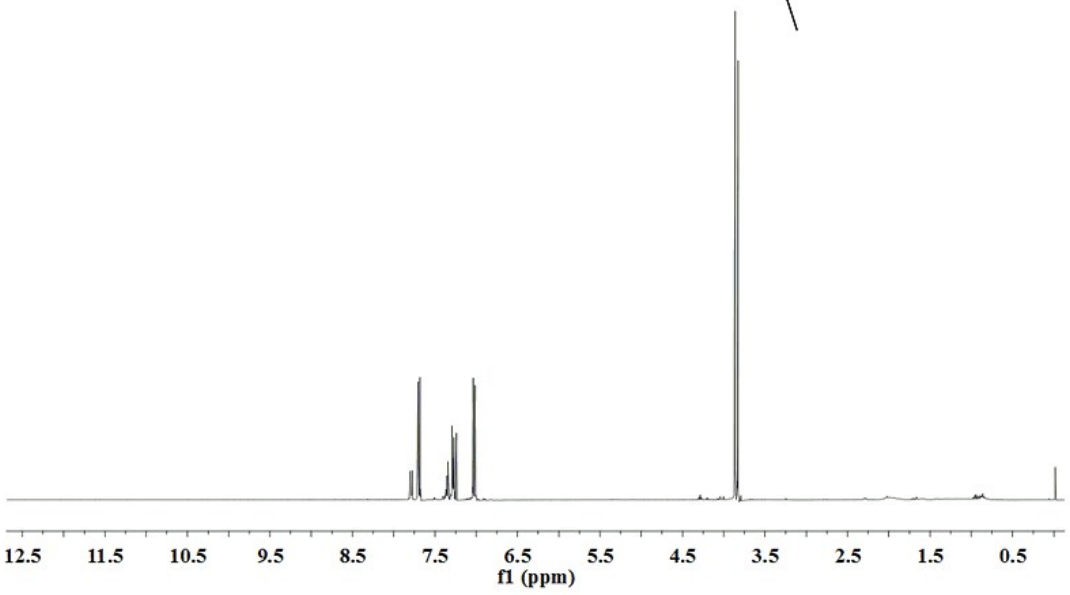
12.5
11.5
10.5
9.5
8.5
7.5
6.5
5.5
4.5
3.5
2.5
1.5
0.5
f1 (ppm)

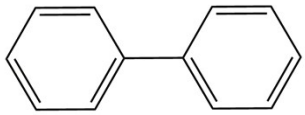

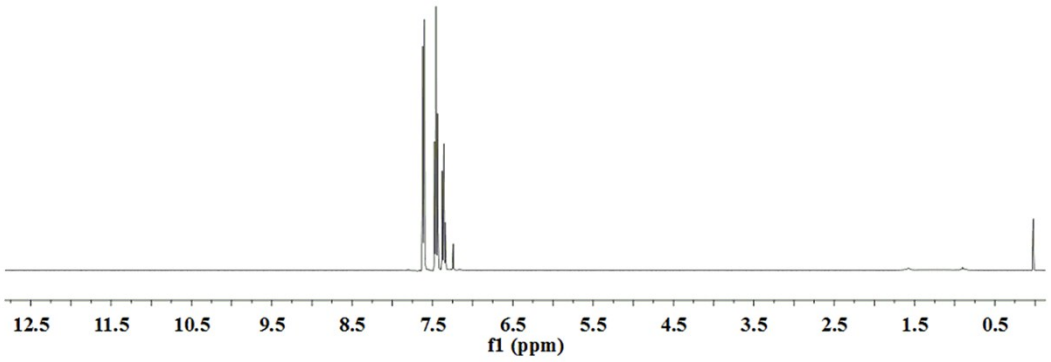
12.5
11.5
10.5
9.5
8.5
7.5
6.5
5.5
4.5
3.5
2.5
1.5
0.5
f1 (ppm)

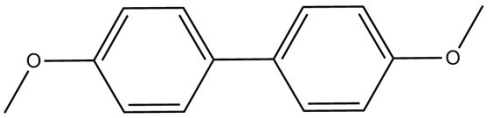
O
O

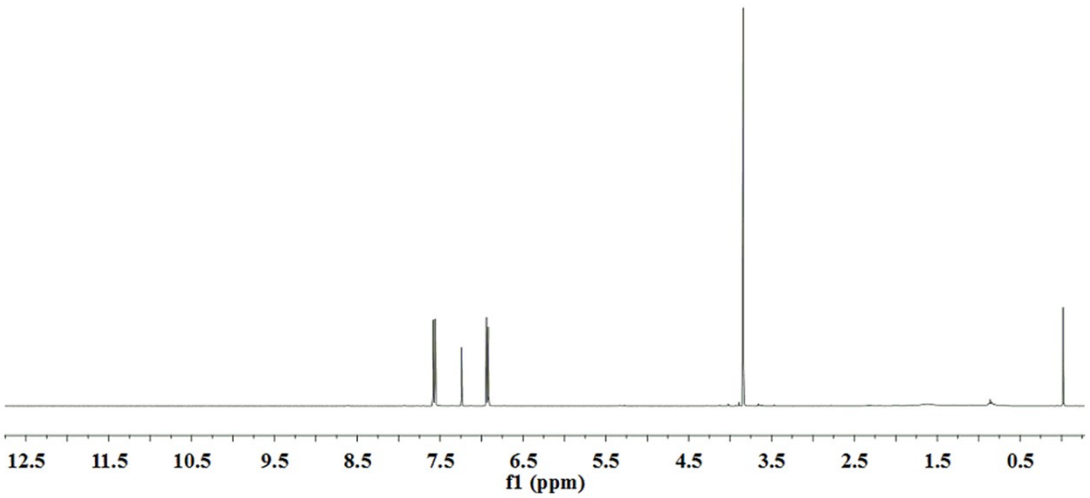
12.5
11.5
10.5
9.5
8.5
7.5
6.5
5.5
4.5
3.5
2.5
1.5
0.5
f1 (ppm)

11. References

(1) (a) H. Lee, S. H. Jung, W. S. Han, J. H. Moon, S. Kang, Y. L. Lee, J. H. Jung and S. Shinkai, *Chem. Eur. J.*, 2011, **17**, 2823-2827; (b) H. Lee, S. Kang, J. Y. Lee and J. H. Jung, *Soft Matter.*, 2012, **8**, 2950-2955.

(2) G. Evindar and R. A. Batey, *J. Org. Chem.*, 2006, **71**, 1802-1808.

(3) S. J. Choi, H. J. Park, S. K. Lee, S. W. Kim, G. Han and P. H. Choo, *Bioorg. Med. Chem.*, 2006, **14**, 1229-1235.

(4) S. Prasenjit, R. Tamminana, P. Nibadita, A. A. Md, P. Rajesh and P. Tharmalingam, *J. Org. Chem.*, 2009, **74**, 8719-8725.

(5) S. Rudrawar, A. Kondaskar and A. K. Chakraborti, *Synthesis.*, 2005, **15**, 2521-2526.

(6) S. Haneda, Z. Gan, K. Eda and M. Hayashi, *Organometallics.*, 2007, **26**, 6551-6555.

(7) J. Canivet, J. Yamaguchi, I. Ban and K. Itami, *Org. Lett.*, 2009, **11**, 1733-1736.

(8) Y. Kawashita, N. Nakamichi, H. Kawabata and M. Hayashi, *Org. Lett.*, 2003, **5**, 3713-3715.

(9) Y. X. Chen, L. F. Qian, W. Zhang and B. Han, *Angew. Chem., Int. Ed.*, 2008, **47**, 9330-9333.

(10) A. Ohsawa, T. Kawaguchi and H. Igeta, *Chem. Pharm. Bull.*, 1982, **30**, 4352-4358.

(11) R. Kumar, C. Selvam, G. Kaur and A. K. Chakraborti, *Synlett.*, 2005, 1401-1404.

(12) J. C. Lewis, J. Y. Wu, R. G. Bergman and J. A. Ellman, *Angew. Chem., Int. Ed.*, 2006, **45**, 1589-1591.

(13) G. Cahiez, A. Moyeux, J. Buendia and C. Duplais, *J. Am. Chem. Soc.*, 2007, **129**, 13788-13789.

(14) G. M. Sheldrick, SHELXS 97, Program for the solution of Crystal Structures, University of Göttingen: Germany, 1997.

(15) Sheldrick, G. M. SHELXS 97, Program for the Refinement of Crystal Structures; University of Göttingen, Germany, 1997.

(16) M. J. Frisch, G. W. Trucks, H. B. Schlegel, G. E. Scuseria, M. A. Robb, J. R. Cheeseman, J. A. Jr. Montgomery, T. Vreven, K. N. Kudin, J. C. Burant, J. M. Millam, S. S. Iyengar, J. Tomasi, V. Barone, B. Mennucci, M. Cossi, G. Scalmani, N. Rega, G. A. Petersson, H. Nakatsuji, M. Hada, M. Ehara, K. Toyota, R. Fukuda, J. Hasegawa, M. Ishida, T. Nakajima, Y. Honda, O. Kitao, H. Nakai, M. Klene, X. Li, J. E. Knox, H. P. Hratchian, J. B. Cross, V. Bakken, C. Adamo, J. Jaramillo, R. Gomperts, R. E. Stratmann, O. Yazyev, A. J. Austin, R. Cammi, C. Pomelli, J. W. Ochterski, P. Y. Ayala, K. Morokuma, G. A. Voth, P. Salvador, J. J. Dannenberg, V. G. Zakrzewski, S. Dapprich, A. D. Daniels, M. C. Strain, O. Farkas, D. K. Malick, A. D. Rabuck, K. Raghavachari, J. B. Foresman, J. V. Ortiz, Q. Cui, A. G. Baboul, S. Clifford, J. Cioslowski, B. B. Stefanov, G. Liu, A. Liashenko, P. Piskorz, I. Komaromi, R. L. Martin, D. J. Fox, T.

Keith, M. A. Al-Laham, C. Y. Peng, A. Nanayakkara, M. Challacombe, P. M. W. Gill, B. Johnson, W. Chen, M. W. Wong, C. Gonzalez and J. A. Pople, Gaussian 03, revision D.01; Gaussian, Inc., Wallingford, CT, 2004.

(17) (a) L. M. Mirica, X. Ottenwaelder and T. D. P. Stack, *Chem. Rev.*, 2004, **104**, 1013-1045; (b) E, A. Lewis and W, B. Tolman, *Chem. Rev.*, 2004, **104**, 1047-1076.

(18) H. Q. Do, O. Daugulis, *J. Am. Chem. Soc.,* 2007, **129**, 12404-12405; (b) Do, H. Q.; Khan, R. M. K.; Daugulis, O. *J. Am. Chem. Soc.,* 2008, **130**, 15185-15192.

(19) K. Shen, Y. Fu, J. Li, L. Liu, Q. Guo, *Tetrahedron.,* 2007, **63**, 1568-1576.